

SUPPLEMENTAL METHODS

Methods

All chemicals and solvents were purchased from commercial sources and used as received without purification unless otherwise noted. The antibody YS5 was prepared by previously described method (1). TFP-PEG₄-TFP_{≥95%} (Catalog ID:11056) was purchase from Biopharma PEG, Watertown, MA, USA. The bifunctional chelators S-2-(4-Isothiocyanatobenzyl)- 1,4,7,10-tetraazacylododecane tetraacetic acid (p-SCN-Bn-DOTA), and 1,4,7,10- tetraazacylododecane tetraacetic acid (DOTA) were purchased from Macrocyclics, Plano, TX. ACS reagent grade of Ammonium acetate (NH₄OAc), and Ethylenediaminetetraacetic acid disodium salt dihydrate (EDTA) were purchased from Sigma Aldrich (St. Louis, MO). Human serum and Rat serum used for stability studies were purchased from Sigma Aldrich. 0.9% sterile saline was obtained from APP Pharmaceuticals. Matrigel matrix and sterile phosphate-buffered saline (PBS), were obtained from VWR. All solutions were prepared using deionized water (≥18 MΩ cm) using Evoqua water purification system. Reactions were monitored by silica gel thin layer chromatography (Whatman UV254 aluminum-backed silica gel). Silica gel (230-400 mesh) used for column chromatography was purchased from Alfa Aesar. Instant thin layer chromatography paper impregnated with silica gel (iTLC-SG) used for radio TLC was purchased from Agilent Technologies, Mississauga, ON, Canada. Macropa.NH₂ was synthesized from a previously described protocol (2).

Analytical Methods

Preparative reverse phase high-performance liquid chromatography (RP HPLC) was performed using the Biotage SP4 system equipped with KP-C18-HS, 35-70 μm, 90 Å (part number: FPL0-1118-16045, Biotage) column using a gradient of 0.1% TFA in H₂O and 0.1% TFA in CH₃CN at a flow rate of 25 mL/min. Analytical chromatography was performed on a Merck Hitachi LaChrom Elite system comprised of an L-2130 Pump, L-2200 autosampler, L-2450 DAD detector, L-2400 UV detector using a Luna C18(2) column, 100 Å, 5 μm, 250 mm x 4.6 mm (Phenomenex, Torrance, CA) at a flow rate of 1.0 mL/min. The gradient used for HPLC method a binary mobile phase that contained 0.1% trifluoroacetic acid (TFA) in H₂O (A) and MeOH (B) or 0.1% formic acid (FA) in H₂O (C) and CH₃CN (D); Method A: 10% B (0-5 min), 10-100% B (5–25 min), 10% B (25-26 min); Method C: 5% D (0-0.5 min), 5% D (0.5–6 min), 5-50% D (6–10 min), 50-95% D (10-15 min), 95-5% D (15-16 min), and 0.1% trifluoroacetic acid in H₂O (C). Liquid chromatography–mass spectrometry (LCMS) was performed using Waters Acquity UPLC QDa mass spectrometer equipped with Acquity Quaternary H Class Solvent Manager, Photodiode Array Detector and

Evaporative Light Scattering Detector. Separations were carried out with Acquity UPLC[®] BEH C18 1.7 mm, 2.1 x 50 mm column at 25 °C, using a mobile phase of water-acetonitrile containing a constant 0.1 % formic acid. ¹H&¹³C-NMR were recorded on a Bruker AV III HD 400 MHz spectrometer using TMS as an Internal standard (0 ppm). The mass analysis was performed at Chemistry Mass Spectrometry Facility, B207 Stanley Hall, QB3 Institute, University of California, Berkeley, CA 94720-3220, on a LTQ FT-ICR mass spectrometer equipped with an electrospray ionization source (Finnigan LTQ FT, Thermo Fisher Scientific, Waltham, MA) operated in either positive or negative ion mode. Matrix-assisted laser desorption/ionization-time of flight (MALDI-TOF) analysis was performed at mass spectrometry core facility, University of Alberta, Edmonton, Canada. Bioscan System AR-2000 Imaging Scanner equipped with winscan software (Bioscan Inc, California, USA) used for radio-TLC analysis. Size-Exclusion Chromatography (SEC) was performed on a Merck Hitachi LaChrom Elite system equipped with Carroll and Ramsey associates model 105S radioactivity detector, 1X PBS buffer as a mobile phase using a column BioSep 5 µm SEC-s3000 290 Å (Phenomenex, Inc. 411 Madrid Ave. Torrance, CA 90501 USA) with a flow rate of 1 mL per minute.

Radiolabeling of DOTA, and Macropa.NH₂ with ²²⁵Ac

37 MBq of ²²⁵Ac(NO₃)₃ was received from Oak ridge national laboratory in solid form, and it was dissolved in 100 mL 0.2M HCl solution. The stock solutions of Macropa.NH₂ (1 mg/mL) and DOTA (1 mg/mL) were prepared in 0.1M NH₄OAc buffer (pH=6.0). An aliquot of ²²⁵Ac(NO₃)₃ in 0.2M HCl (185 KBq, 0.83 µL) was added to a solution of Macropa.NH₂ (32 µg, 32 µL) diluted in 0.1M NH₄OAc, pH=6.0. The reaction solution was incubated at 25 °C for 30 min and analyzed by radio TLC over Silica plates (1.05554.0001, Millipore, MA, USA) using 0.4M sodium citrate (pH=5.5) as the eluent, which confirmed >95% radiochemical yield. Similarly, ²²⁵Ac-DOTA complex was prepared by incubating the DOTA (14.1 µg, 14.1 µL) with ²²⁵Ac(NO₃)₃ in 0.2M HCl (18.5 KBq, 0.83 µL) 0.1M NH₄OAc, pH=6.0 at 85 °C. The radio TLC was confirmed the >95% radiochemical yield. Both the reactions were diluted in saline (900 µL). 100 µL (~18.5 MBq) of ²²⁵Ac-Macropa.NH₂/DOTA were injected intravenously to healthy wildtype C57BL/6 mice.

Stability studies

¹³⁴Ce-Macropa.NH₂ was synthesized using the 10:1 (L:M) ratios. The molar ratios (0.5:1-10:1, ligand versus metal) of Macropa.NH₂ and DOTA were determined using the stable element content of Ce (1.83 µg/mL) and La (2.00 µg/mL) in the solution as per the certificate of analysis sent by Los Alamos National Laboratory (Supplemental Figure 1). The purity of the complex was confirmed by radio TLC (>95%) was diluted separately with PBS buffer, Saline, Human serum,

and Rat serum (90% designated buffer concentration) and the samples were incubated at 37 °C over 7 days. The decomplexation was monitored by radio TLC. The plates were developed with C18, 10% NH₄Cl: MeOH (1:1) as the eluent. Under these conditions, free ¹³⁴Ce(R_f=0) remained at the baseline while the intact conjugate migrated to R_f=0.53.

Cell culture

22Rv1 prostate cancer cells were provided by American Type Culture Collection. The cells were cultured with RPMI medium supplemented with 10% fetal bovine serum, 1% penicillin, and streptomycin in a CO₂ incubator at 37 °C.

In vitro cell binding assay

22Rv1 cells were seeded in six-well plate at the density of 1x10⁶ cells per well. To avoid non-specific binding, 1% non-fat milk was added to the cells and 10-fold excess of cold PSMA was added to the cells for blocking control and incubated for 1 hour. Following this, cells were treated with various concentrations of ¹³⁴Ce-PSMA-617 (0.01, 0.02, 0.04 and 0.8 nM) further incubated for one hour. Then, cells were washed with PBS twice, and 5 N NaOH was added to the wells. Cell lysates were collected in collection tubes, and counted on the HIDEX gamma counter.

In vitro K_d measurement

A saturation binding assay was performed on 22Rv1 cells. Cells were seeded (1 million cells per well) in six-well plates and were allowed to attach overnight. Following this, cells were incubated with 1% non-fat milk for one hour to avoid non-specific binding. Next, cells were treated with the range of concentrations of ¹³⁴Ce-Macropa-PEG₄-YS5 (0.01, 1, 3, 5, 10, and 12 nM) in triplicate for one hour. Finally, to remove the unbound activity, cells were washed with PBS three times, lysed with 5N NaOH, and the amount of the ¹³⁴Ce-Macropa-PEG₄-YS5 and ¹³⁴Ce-PSMA-617 bound to the cells was measured on HIDEX gamma counter by taking appropriate standards. To find the K_d values, data from the gamma counter was fitted into a non-linear equation for one-site-specific binding using the GraphPad Prism program.

CD46 magnetic beads target binding fraction assay

Magnetic beads target binding assay was carried out using our previously described method (3).

Xenograft models

All procedures used in animal studies were conducted according to Institutional Animal Care and Use Committee–approved guidelines at the Laboratory Animal Resource Center (LARC) at the

University of California, San Francisco (San Francisco, CA). 5-6-week-old male athymic nu/nu mice were purchased from the Jackson laboratory (Strain: 002019, Homozygous) and housed under aseptic conditions. A suspension of 2.5 million 22Rv1 cells in a mixture of PBS buffer and Matrigel (1:1) was inoculated subcutaneously into the right flank of the mice. Animals underwent PET imaging, as well as biodistribution analysis when the tumor reached a size of 100-200 mm³.

PET imaging methods

Since ¹³⁴Ce decays to ¹³⁴La via electron capture, and ¹³⁴La emits positrons for PET imaging, PET acquisition was configured for ¹³⁴Ce's half-life (3.16 d) and the positron branching ratio (63%) for quantitative purposes. For dynamic imaging, PET data was acquired in list mode and was processed to produce a total of 42 dynamic multiframes (24 x 10 s, 12 x 30 s and 6 x 330 s). PET imaging data were acquired in list mode and reconstructed using an iterative 2D OSEM reconstruction algorithm provided by the manufacturer with both attenuation and scatter corrections applied. The resulting image data were then normalized to the administered activity to parameterize images in terms of %ID/mL. Open-source Amide software is used for processing the images obtained from the PET/CT. PET images were acquired following CT acquisition for co-registration and attenuation correction.

Ex-vivo Biodistribution Analysis

All mice used in this study were euthanized via cervical dislocation under isoflurane anesthesia. Wild-type C57BL/6 male mice and 22Rv1 tumor-bearing mice were sacrificed at designated time points post-injection of ¹³⁴Ce/AcCl₃, ¹³⁴Ce/²²⁵Ac-Macropa.NH₂, ¹³⁴Ce/²²⁵Ac-DOTA, and ¹³⁴Ce/²²⁵Ac-Macropa-PEG₄-YS5. A dose of 18.5 KBq of actinium-labeled conjugates was used for the study. Blood was collected through cardiac puncture. All the other major organs such as the liver, heart, kidney, lung, spleen, stomach, small intestine, large intestine, brain, muscle, bone, blood, and tumor were collected, weighed, and counted in an automated Gamma Counter (Hidex) using energy windows 450-580 KeV (for ¹³⁴Ce) and 50-500 KeV (for ²²⁵Ac). The counts were decay corrected with the time of Injection and then the percent injected dose per gram (%ID/g) was calculated by comparison with known radioactivity standards.

Statistical Analysis

All data were expressed as mean ± SD. Data were analyzed using GraphPad prism 8 and P value < 0.05 were considered statistically significant.

Certificate of Analysis

Cerium-134

Batch ID 22-8-1-Ce134
 Release Date Aug 18, 2022 Calibration date, Time Aug 24, 12:00 ET
 Expiration date, time Sept 10, 2022 12:00 ET

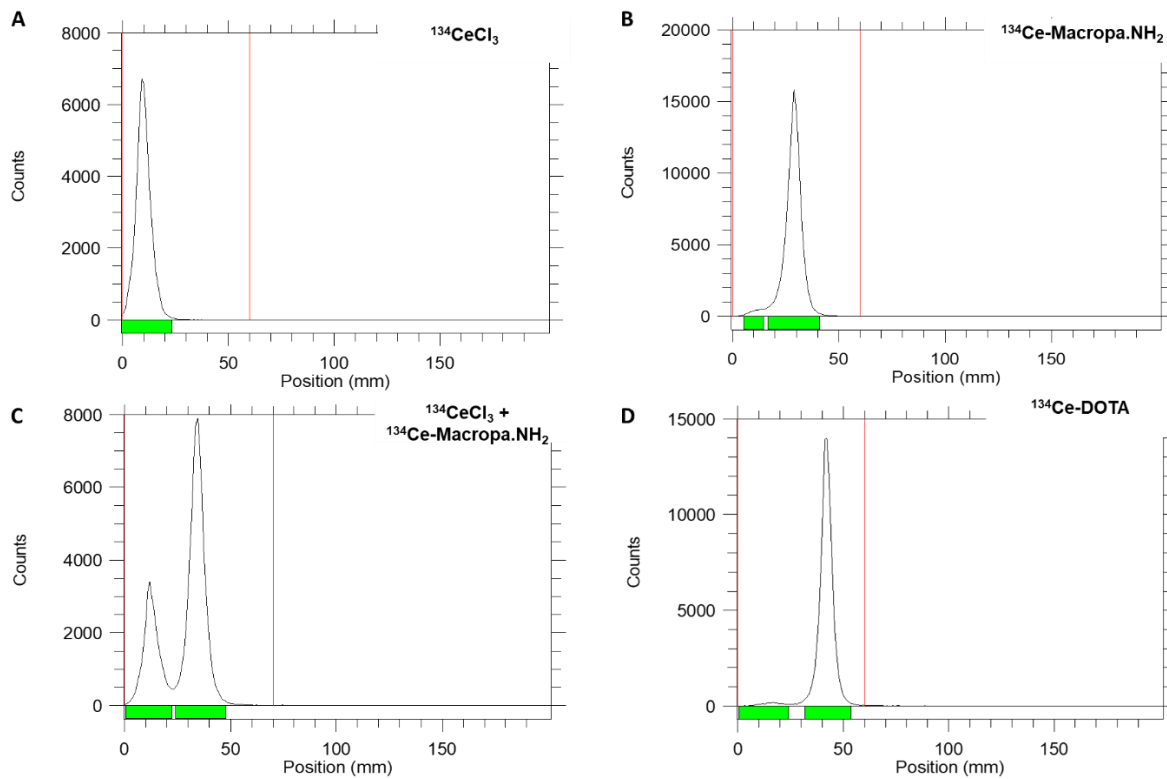
Property	Description	Test results decayed to Calibration date
Chemical Form	Ce (III) in 0.1 M HCl	N/A
Activity concentration of primary isotope	Ce-134 quantified from the 162.3 keV gamma emission	19.35 mCi/mL
Specific Activity	Determined by ICP-OES	10574 Ci/g
Activity concentration of minor isotopes	Ce-137m = 0.45 mCi/ml	Ce-139 = 0.22 mCi/ml
	Ce-135 = 0.01 mCi/ml	

Stable element content (if applicable):
 Ce = 1.83 ug/mL, La = 2.00 ug/mL, Na = 4.24 ug/mL, Ca = 1.64 ug/mL
 Notes, Comments
 Reviewed by: Heath Wade Digitally signed by Heath Wade
Date: 2022.08.22 08:11:55 -0600

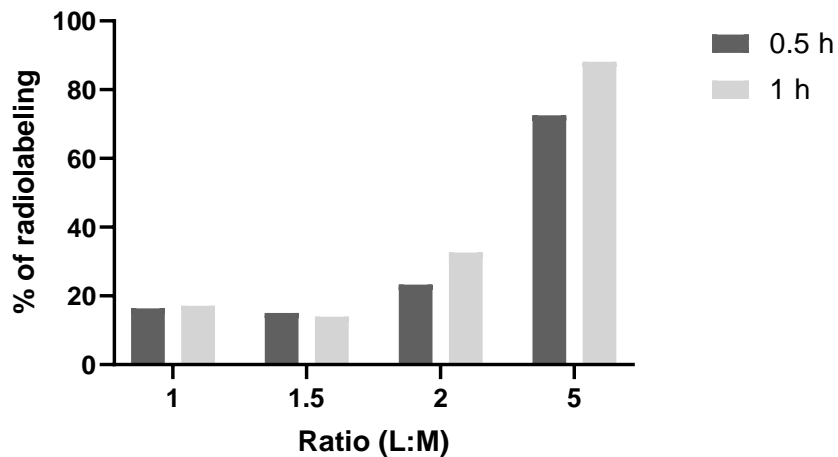
The information above is accurate and the batch has been approved for release.

Name: Veronika Mocko Title: QA Officer (Acting) Contact: vmocko@lanl.gov
 Signature: Veronika Mocko Digitally signed by Veronika Mocko
Date: 2022.08.19 17:07:49 -0600 Date: 08/19/2022

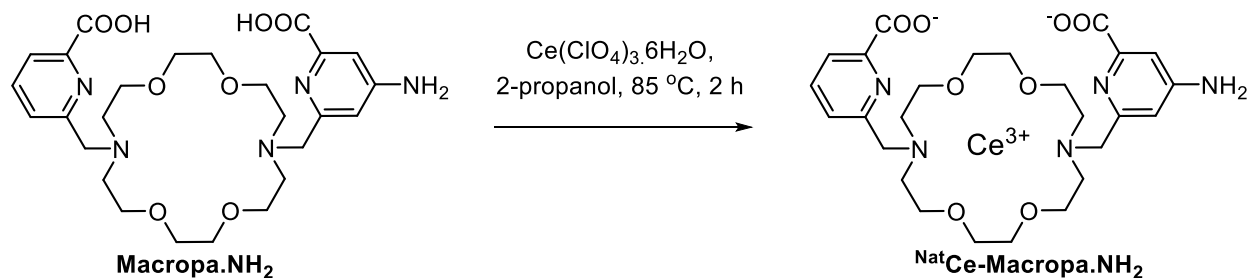
SUPPLEMENTAL FIGURE 1. Certificate of analysis for ¹³⁴Ce, showing the stable metal contents of Ce and La.



SUPPLEMENTAL FIGURE 2. Radiolabeling of Macropa.NH₂ and DOTA, 10:1 ratios of Ligand to metal. C18 Radio-TLC of ¹³⁴CeCl₃ (A), ¹³⁴Ce-Macropa.NH₂ (B), ¹³⁴CeCl₃ co-spot with ¹³⁴Ce-Macropa.NH₂ (C), and ¹³⁴Ce-DOTA (D).

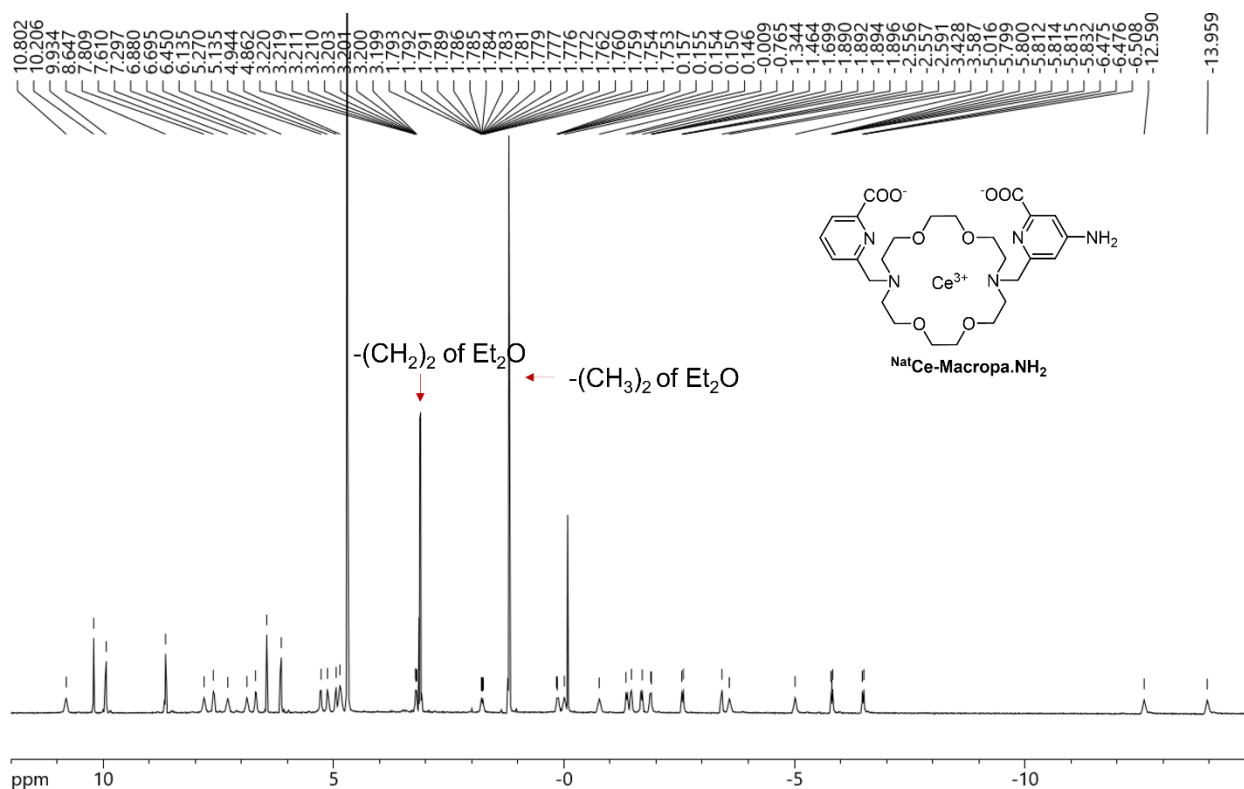


SUPPLEMENTAL FIGURE 3. Radiolabeling of DOTA at 60 °C for 30 min and 1 h, n=1; radiolabeling was monitored by radio TLC.

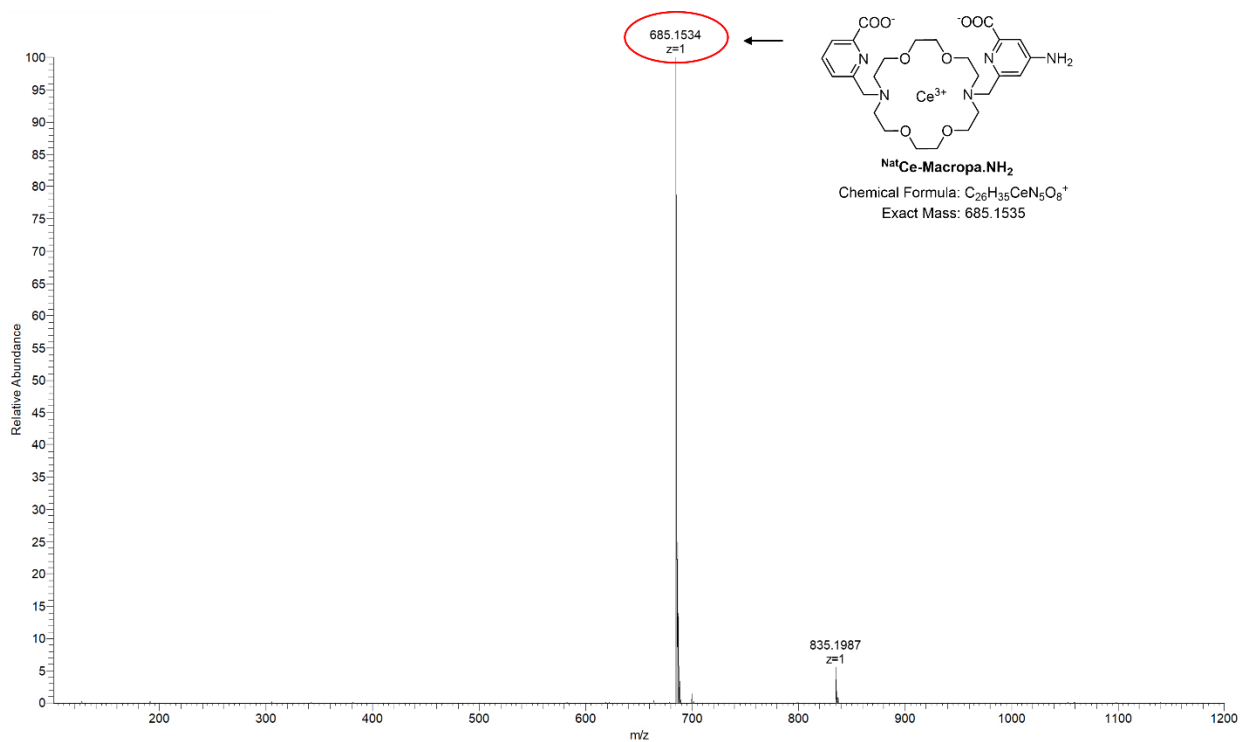


Supplemental Reaction Scheme 1: Synthesis of ^{Nat}Ce-Macropa.NH₂

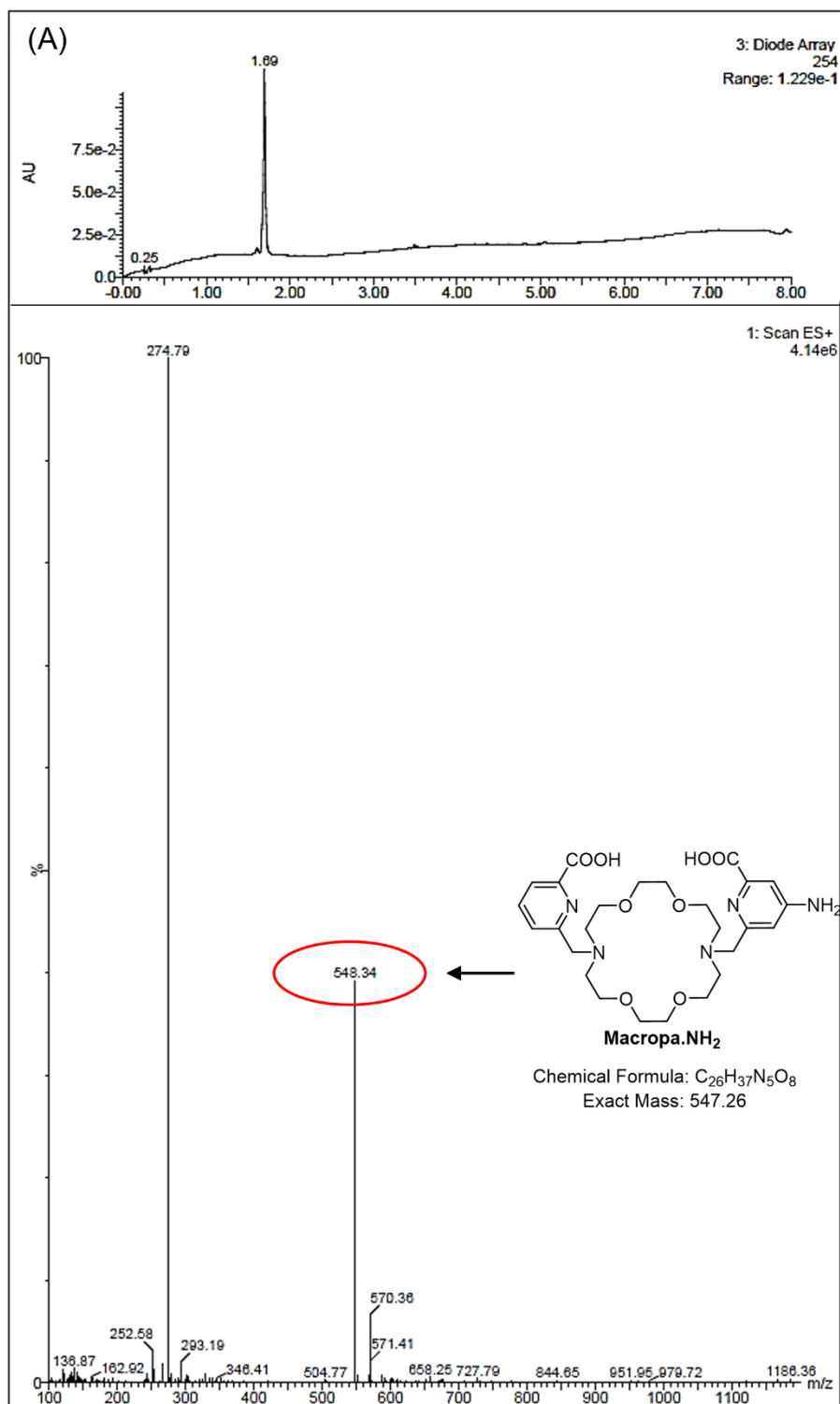
Triethylamine (29 μL , 0.20 mmol) was added to a suspension of Macropa.NH₂.4TFA (50 mg, 0.05 mmol) in 2-propanol (0.6 mL) at room temperature. Then, A solution of $\text{Ce}(\text{ClO}_4)_3 \cdot 6\text{H}_2\text{O}$ (41 mg, 0.075 mmol) in 2-propanol (0.5 mL) was added dropwise to the above solution at 85 °C, a precipitate formed immediately and stirred for 2 h at 85 °C. The cream suspension was centrifuged, the supernatant was removed, and the solid was washed with 2-propanol (2 \times 1 mL) followed by diethyl ether (2 \times 1 mL) and then air-dried on filter paper to give the title complex as a pale-tan solid (21 mg, 61.76%) containing traces of diethyl ether. ¹H NMR (400 MHz, D₂O-d₆): δ = 10.82 (Bs), 10.20 (s), 9.93 (s), 8.64 (s), 7.80 (s), 7.61 (s), 7.29 (s), 6.88 (s), 6.69 (s), 6.45 (s), 6.13 (s), 5.27 (s), 5.13 (s), 4.94 (s), 4.86 (s), 3.22-3.19 (m), 1.79-1.75 (m), 0.15-0.14 (m), 0.009 (s), -0.76 (s), -1.34 (s), -1.46 (s), -1.69 (s), -1.89 (s), -2.55 - -2.59 (m), -3.42 - -3.58 (m), -5.01 (s), -5.79 - -5.83 (m), -6.47 - -6.50 (m), -12.59 (bs), -13.95 (bs); HRMS (m/z): 685.1534 [M⁺]; Calc: 685.1535.

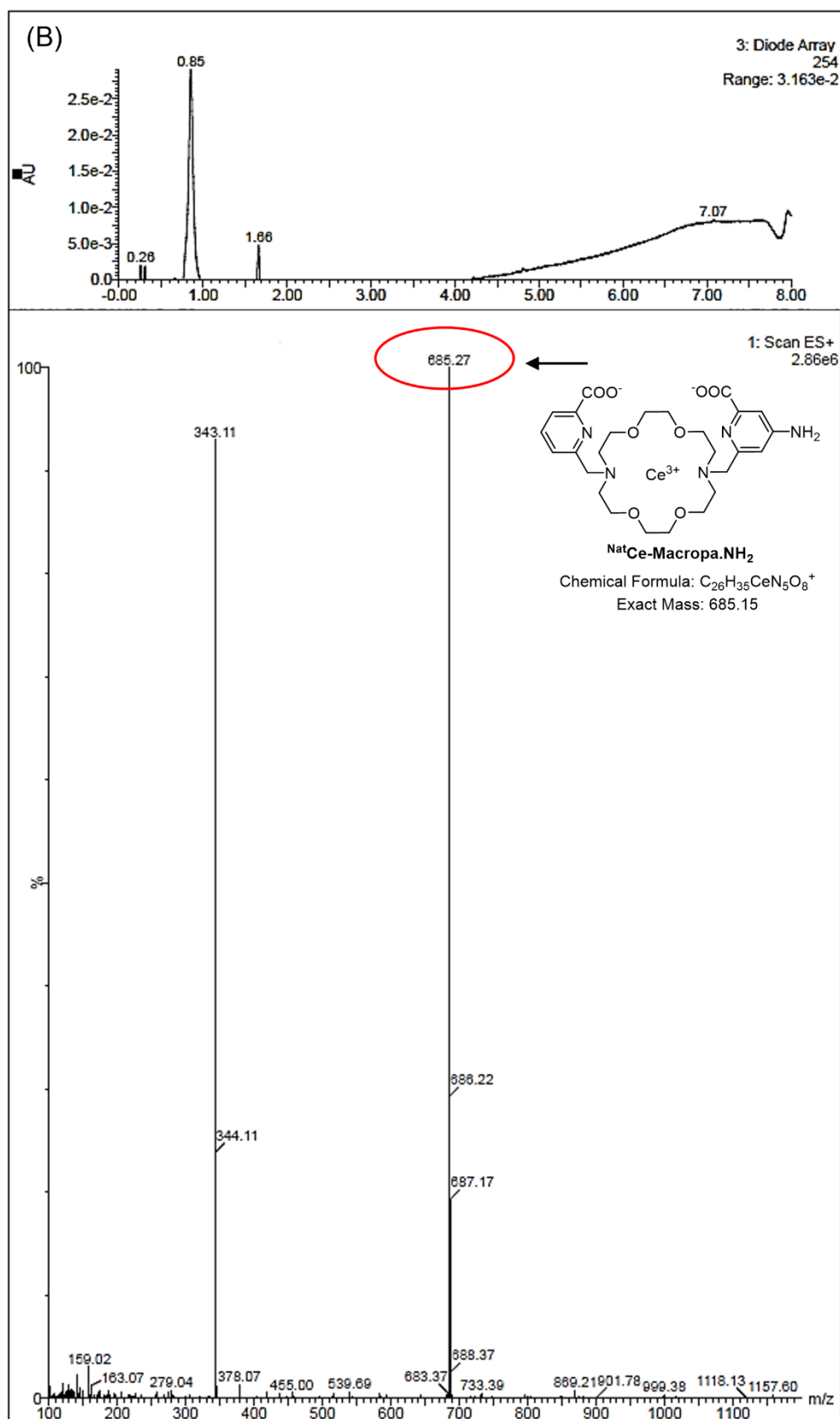


Supplemental Figure 4. $^1\text{H-NMR}$ of $^{\text{Nat}}\text{Ce-Macropa.NH}_2$ in D_2O (400 MHz) with traces of diethyl ether; $^{\text{Nat}}\text{Ce-Macropa.NH}_2$ complex is a paramagnetic therefore the $^1\text{H-NMR}$ peaks shows broadening and negative ppm values.

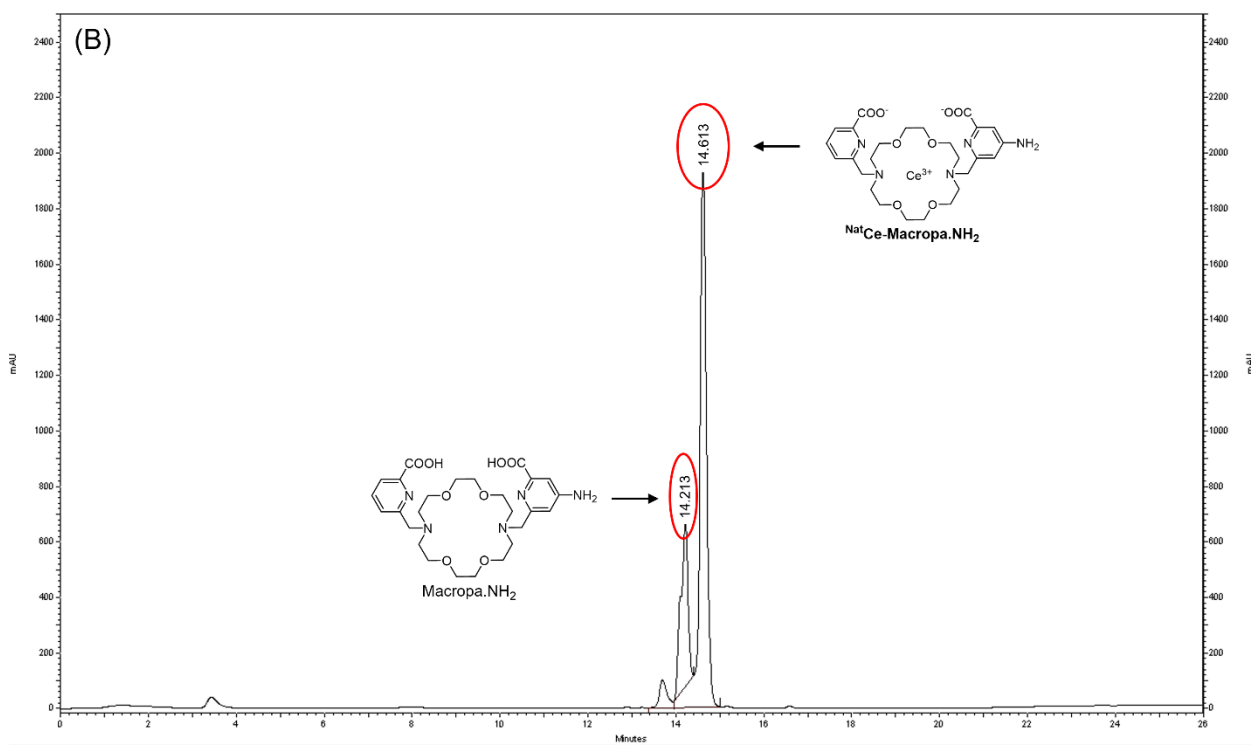
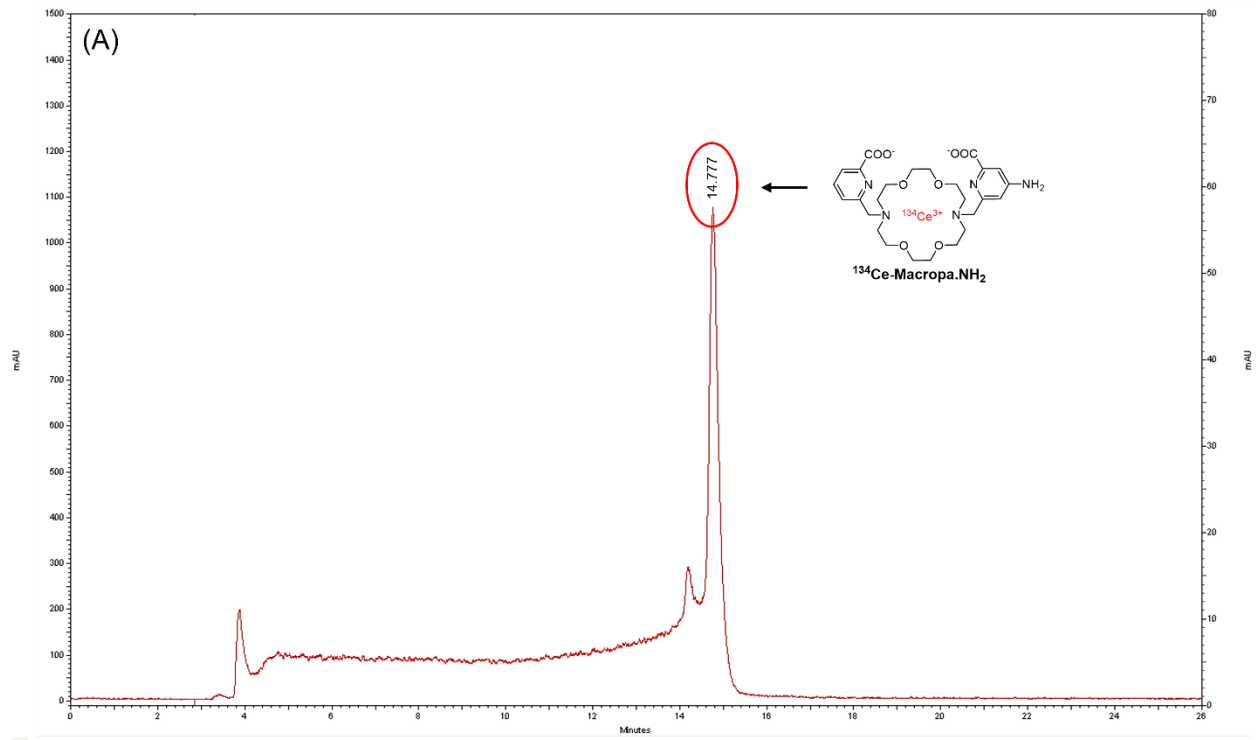


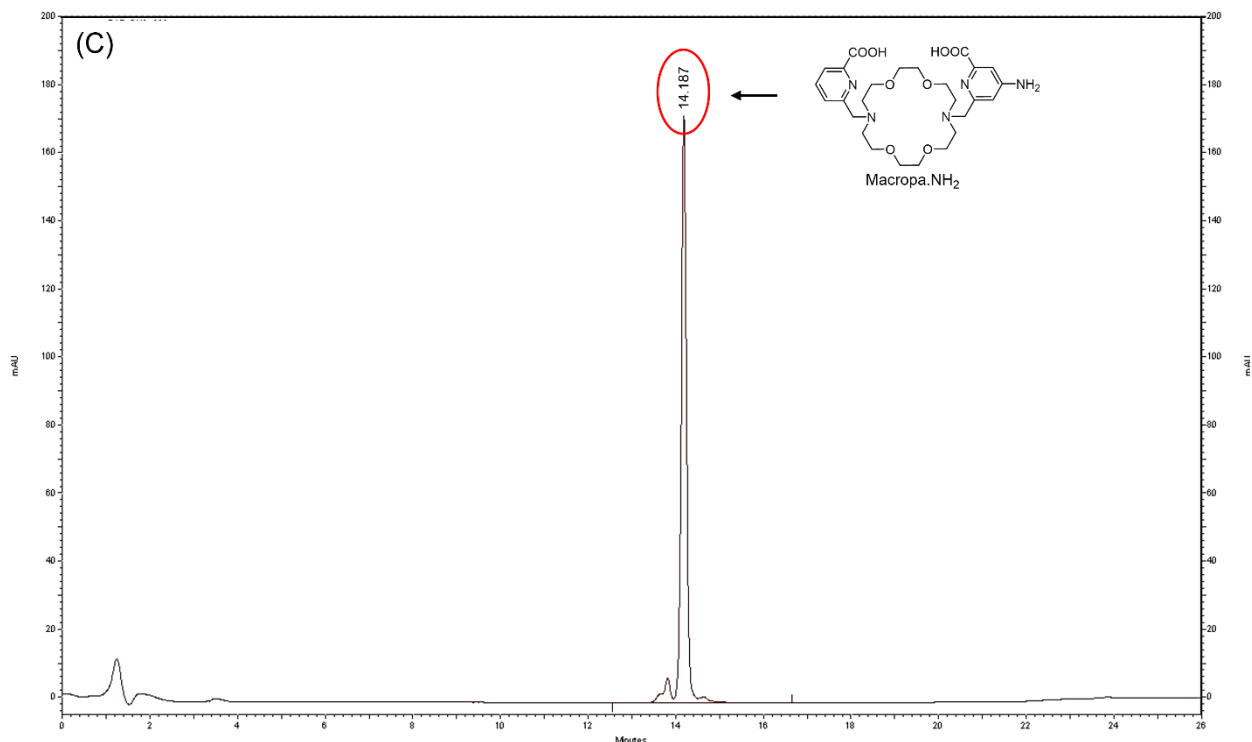
Supplemental Figure 5. HRMS of $\text{NatCe-Macropa.NH}_2$ complex.



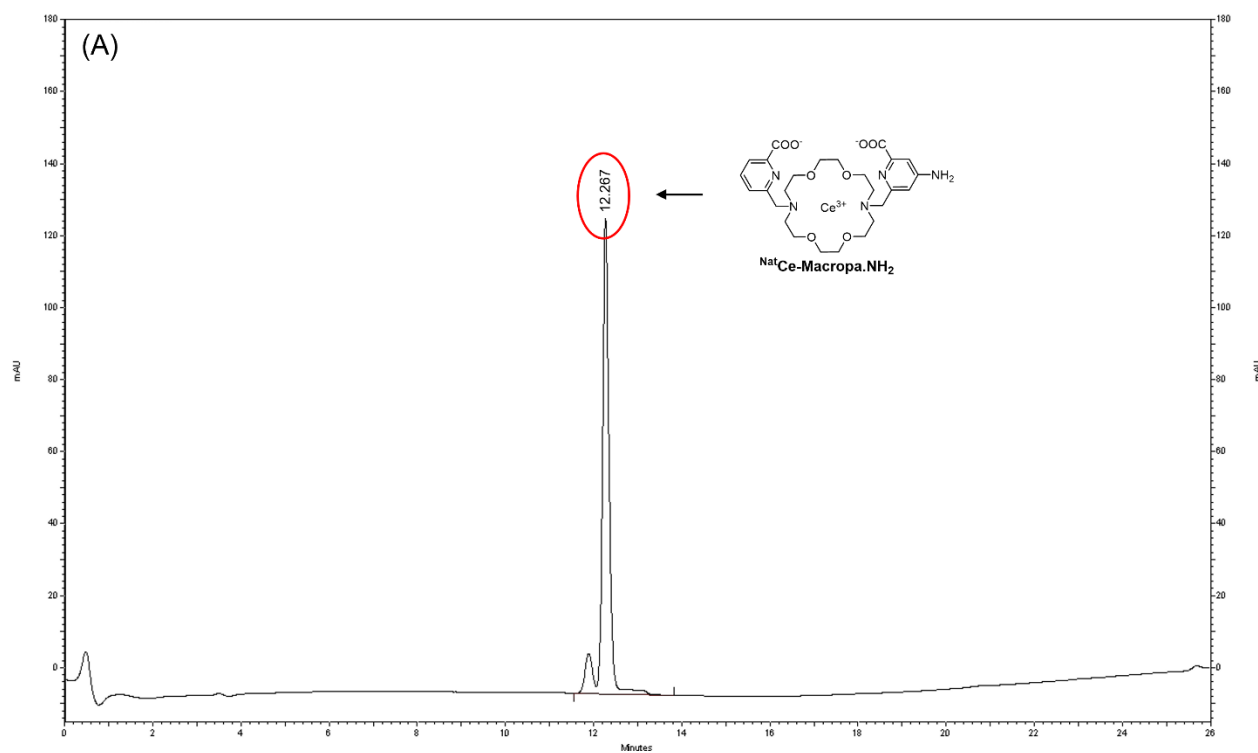


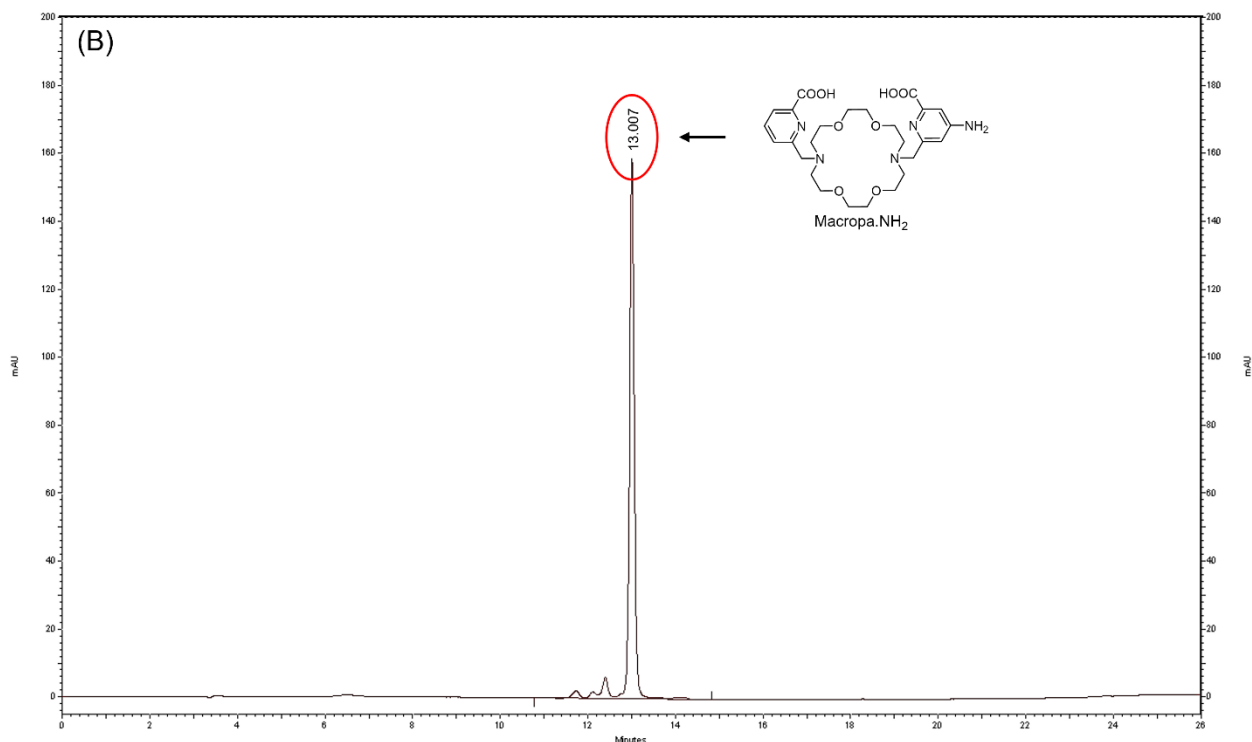
Supplemental Figure 6. LCMS of Macropa.NH_2 and $^{134}\text{Ce-Macropa.NH}_2$.



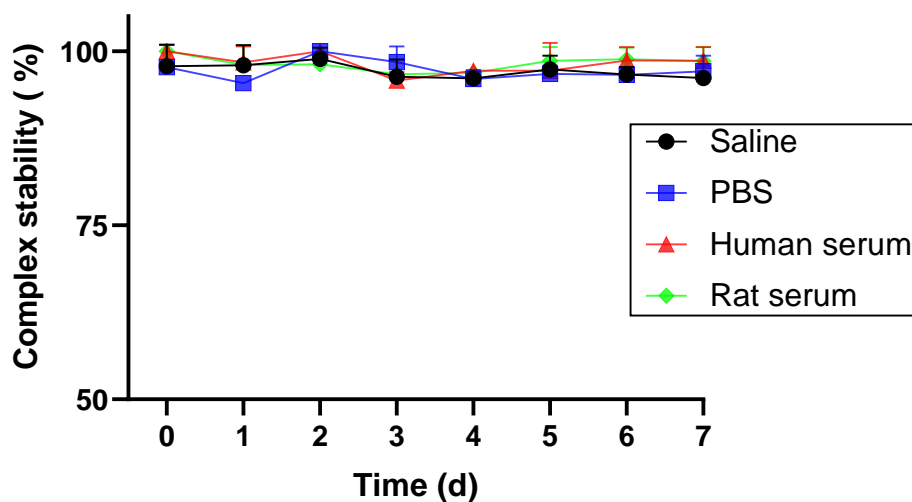


Supplemental Figure 7. A radio-HPLC chromatogram of ¹³⁴Ce-Macropa.NH₂ (A, R_t = 14.777). UV-HPLC chromatogram of ^{Nat}Ce-Macropa.NH₂ (B, R_t = 14.613) is unstable under 0.1% trifluoroacetic acid conditions and Macropa.NH₂ (C, R_t = 14.187). Method A with 0.1% TFA in H₂O

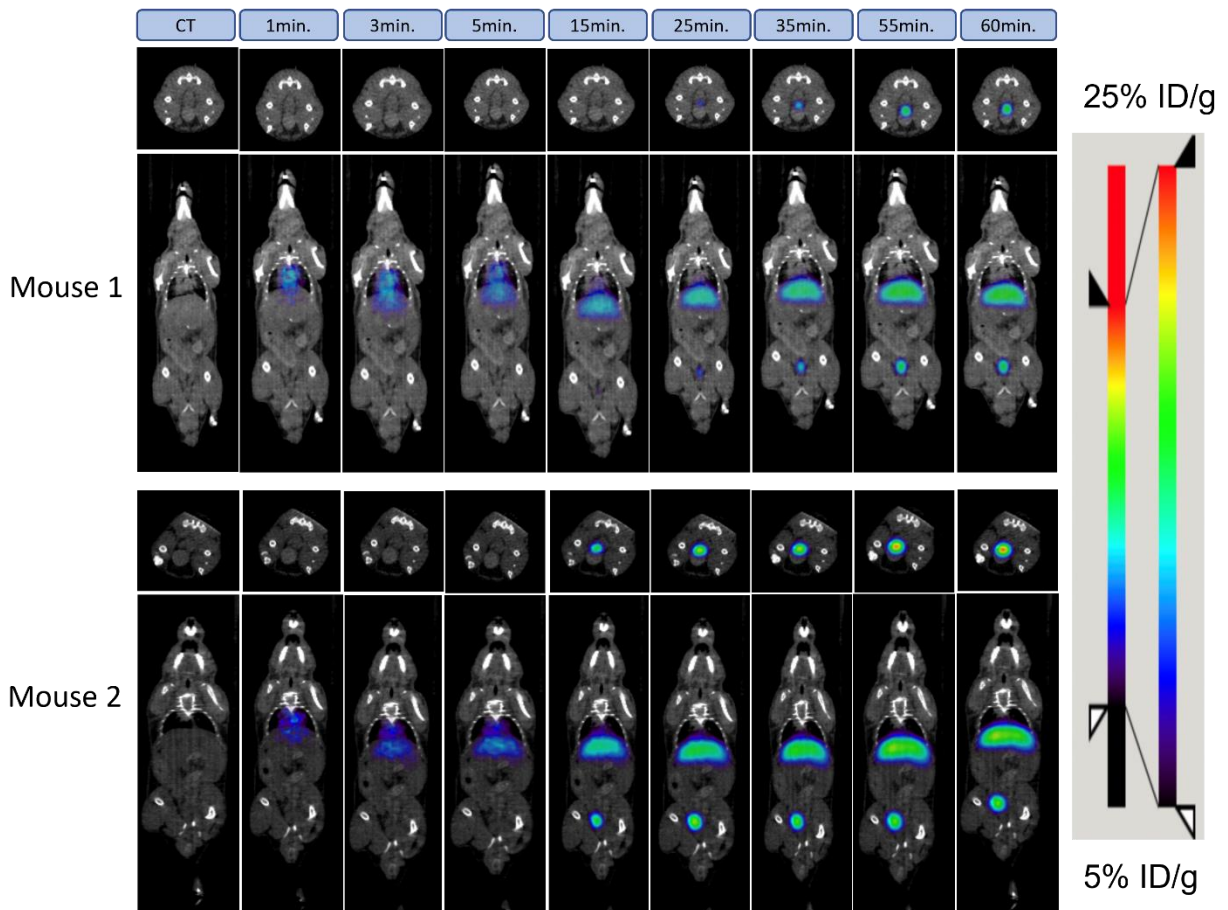




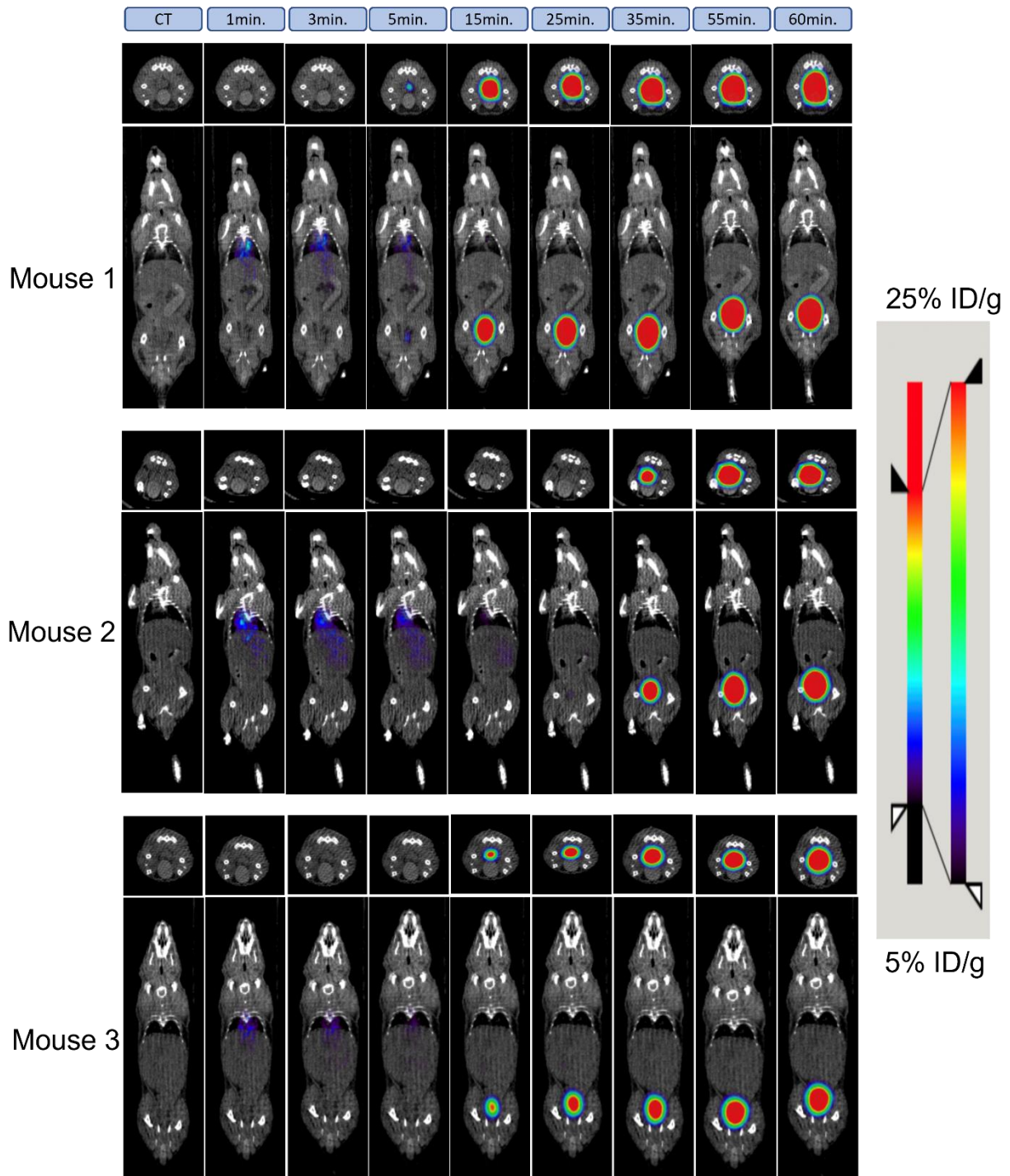
Supplemental Figure 8. UV-HPLC chromatogram of $^{Nat}\text{Ce-Macropa.NH}_2$ (A, $R_t = 12.267$) and Macropa.NH_2 (B, $R_t = 13.007$); the $^{Nat}\text{Ce-Macropa.NH}_2$ complex is stable under 0.1% formic acid conditions. Method A with 0.1% FA in H_2O



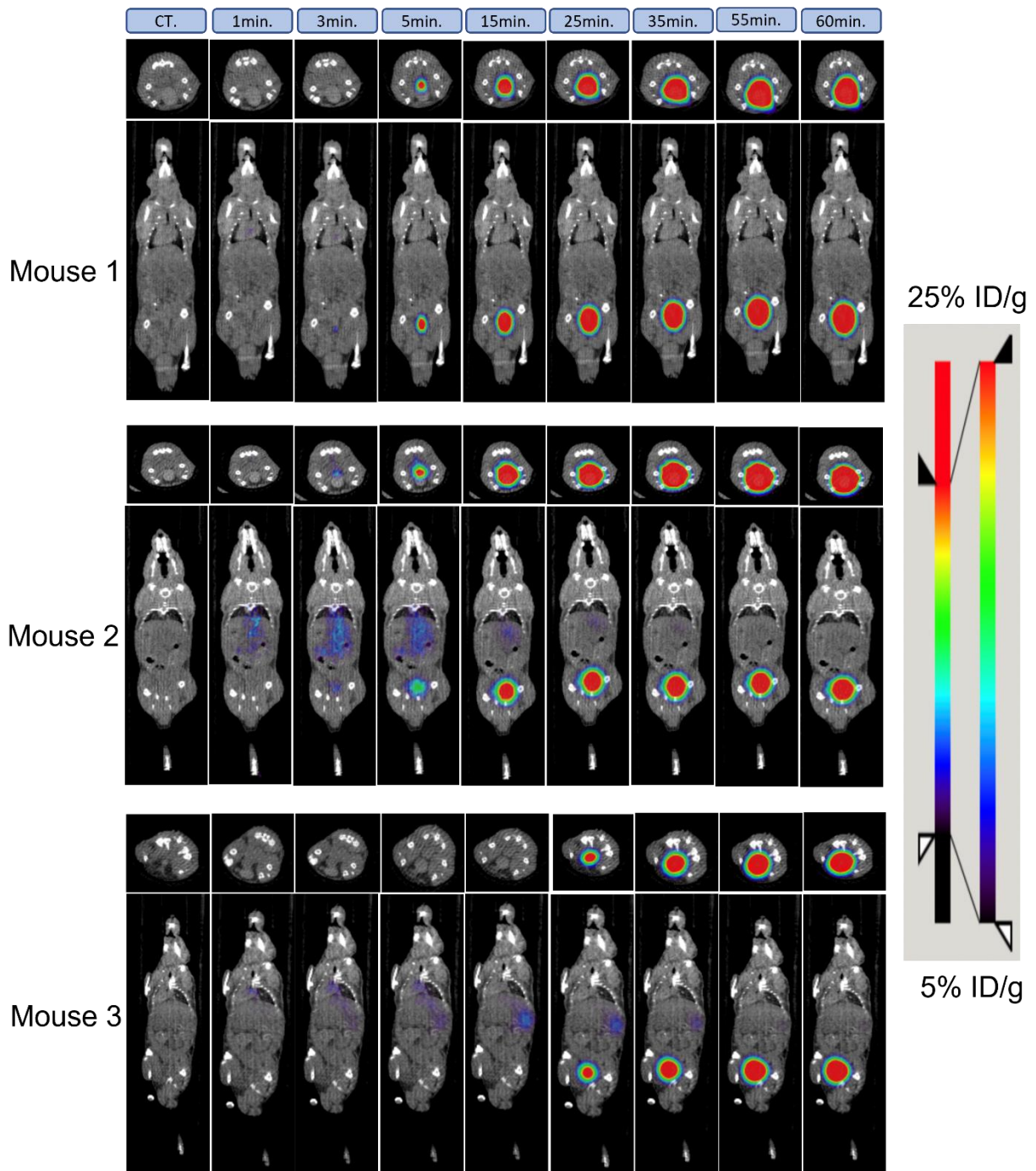
SUPPLEMENTAL FIGURE 9. Stability of $^{134}\text{Ce-Macropa.NH}_2$ at 37°C for 7 days ($n=2$ for each condition).



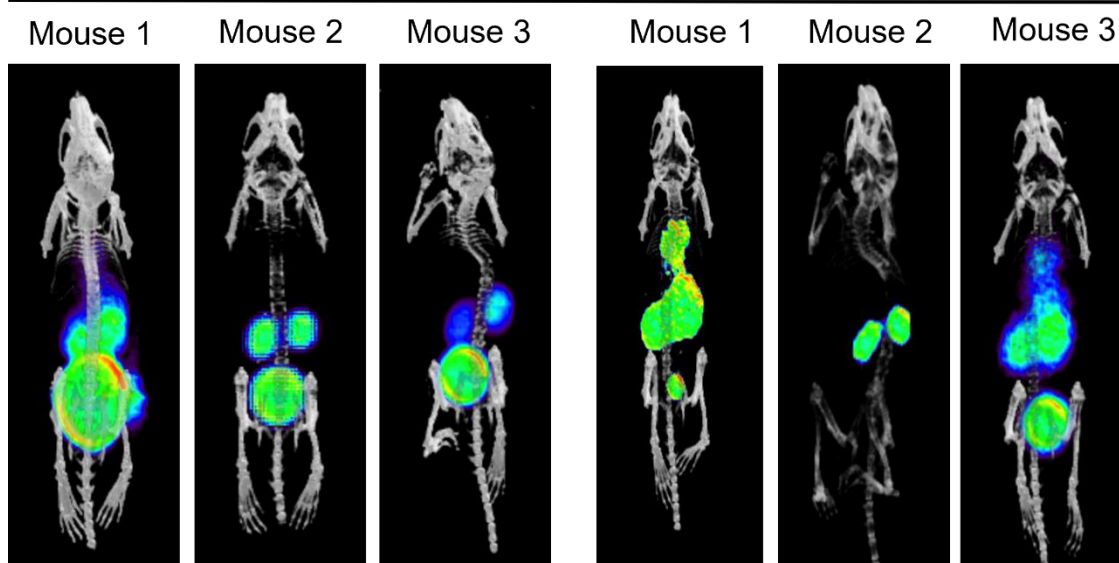
SUPPLEMENTAL FIGURE 10. Dynamic coronal fused μ PET/CT images obtained after injection of free $^{134}\text{CeCl}_3$ in healthy wild type C57BL/6 mice over 1 h (n=2)



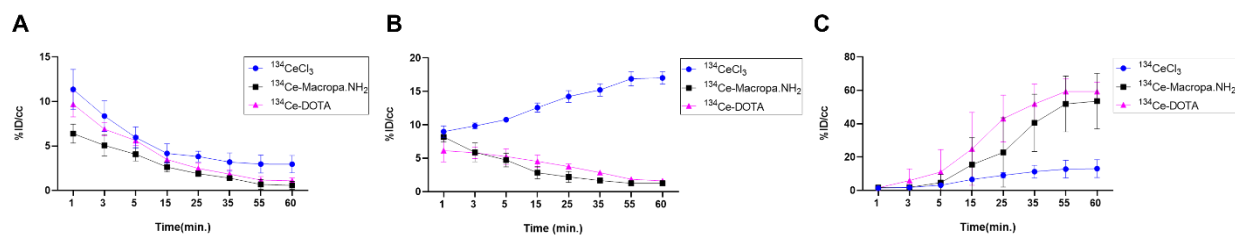
SUPPLEMENTAL FIGURE 11. Dynamic coronal fused μ PET/CT Images obtained after injection of ^{134}Ce -Macropa.NH₂ in healthy wild type C57BL/6 mice over 1 h (n=3).



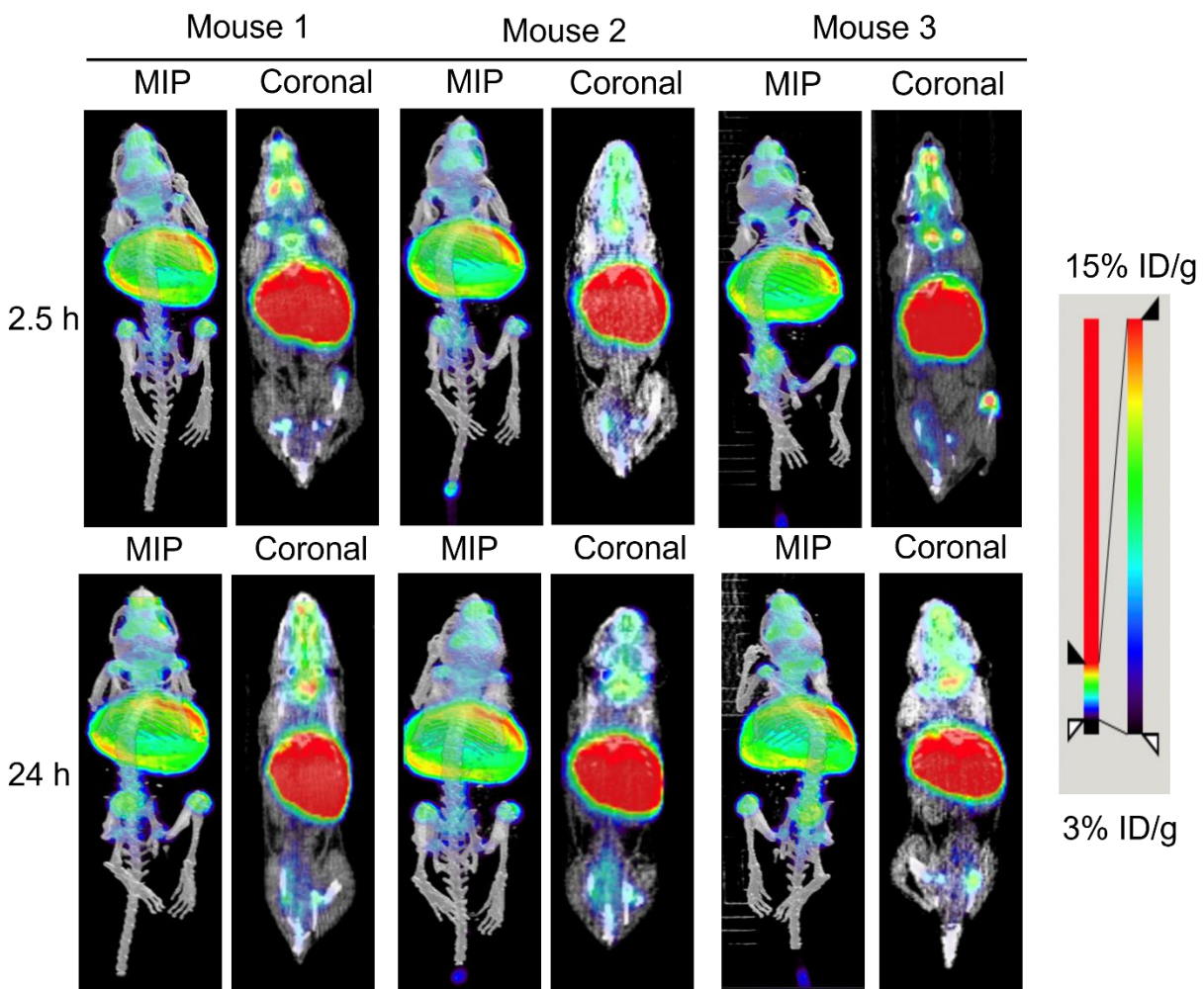
SUPPLEMENTAL FIGURE 12. Dynamic coronal fused μ PET/CT Images obtained after injection of ^{134}Ce -DOTA in healthy wild-type C57BL/6 mice over 1 h (n=3).



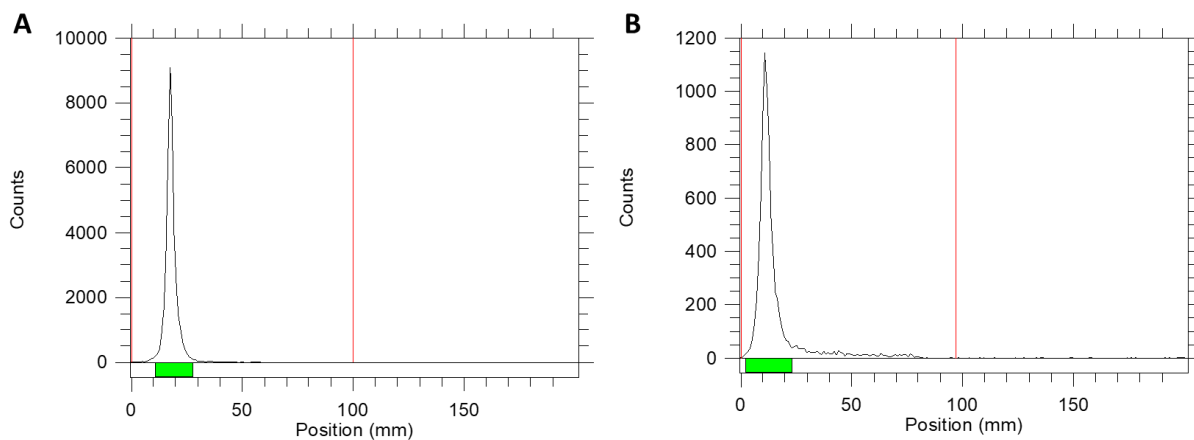
SUPPLEMENTAL FIGURE 13. Volume rendered Maximum-intensity projection (MIP) $\mu\text{PET/CT}$ Images of dynamic scans at 1 h in healthy wild type C57BL/6 mice Injcted intravenously with $^{134}\text{Ce-Macropa.NH}_2$ and $^{134}\text{Ce-DOTA}$ ($n=3$).



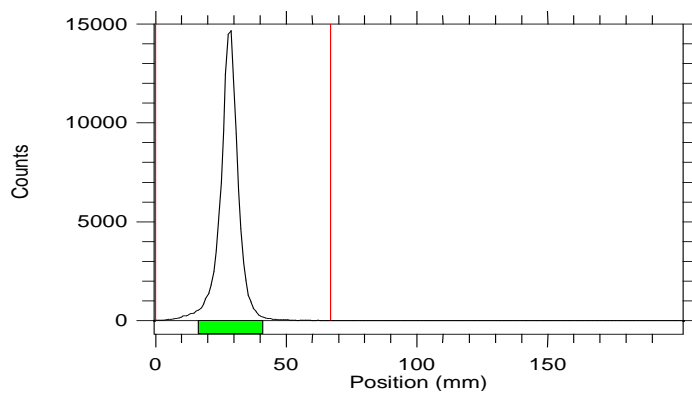
SUPPLEMENTAL FIGURE 14. Time activity curves generated through region of interest analysis for dynamic μPET images of $^{134}\text{CeCl}_3$, $^{134}\text{Ce-Macropa.NH}_2$ and $^{134}\text{Ce-DOTA}$ in healthy wild type C57BL/6 mice ($n=3$) ($n=2$ for $^{134}\text{CeCl}_3$). Blood (A), Liver (B) and Bladder (C).



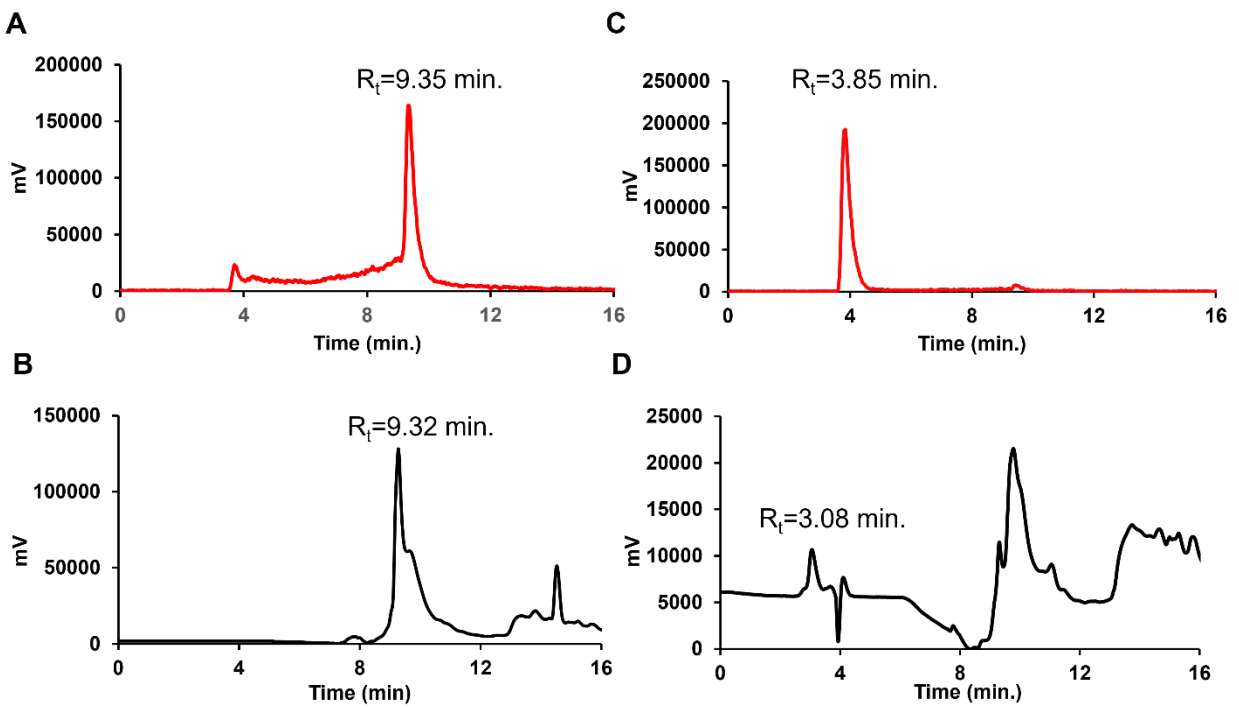
SUPPLEMENTAL FIGURE 15. Maximum-intensity projection (MIP) μ PET/CT Images of healthy wild type C57BL/6 mice injected with $^{134}\text{CeCl}_3$. Images obtained at 2.5 h and 24 h post injection (p.i.) (n=3).



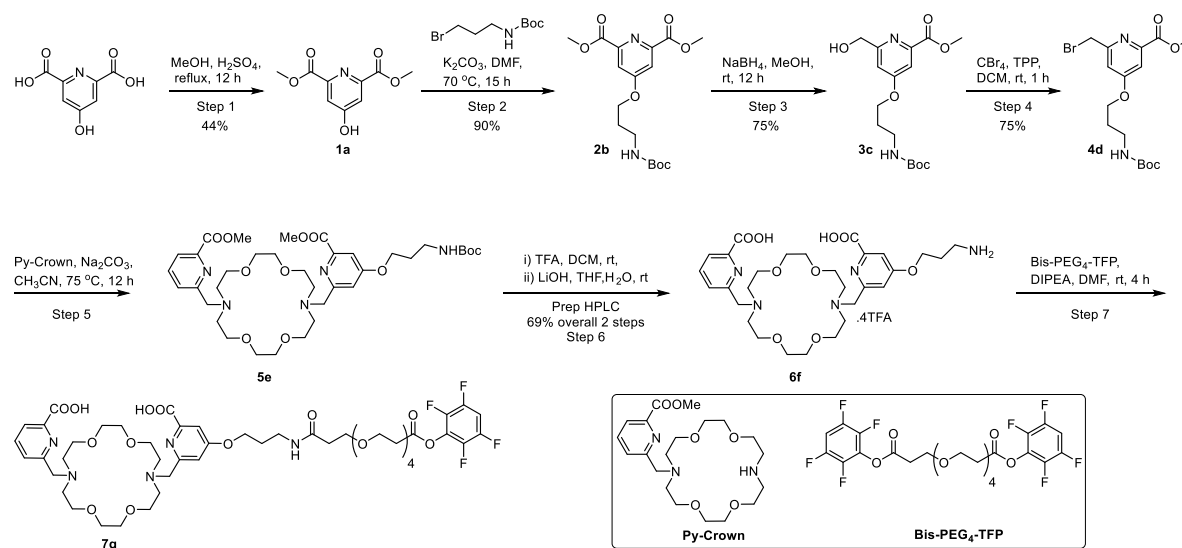
SUPPLEMENTAL FIGURE 16. Radiolabeling of Macropa.NH₂ and DOTA with ²²⁵Ac(NO₃)₃ in 0.2M HCl. Radio TLC of ²²⁵Ac-Macropa.NH₂ (A) and ²²⁵Ac-DOTA (B), eluted with 0.5M Sodium citrate buffer, pH=5.5 on silica plates.



SUPPLEMENTAL FIGURE 17. Radiolabeling of PSMA-617 at 60 °C using 10:1 Ligand to metal ratios. Radio C18 TLC eluted with 10% NH₄Cl:MeOH(1:1).



SUPPLEMENTAL FIGURE 18. Radioactive (A) and 254 nm UV (B) HPLC chromatogram of $^{134}\text{Ce-PSMA-617}$. Radioactive (C) and 254 nm UV (D) chromatogram of $^{134}\text{CeCl}_3$.



Supplemental Reaction Scheme 2: Synthesis of the bifunctional chelator Macropa-PEG₄-TFP ester (**7g**). Briefly, the esterification of chelidamic acid afforded the corresponding dimethyl ester (**1a**). Intermediate **1a** was alkylated with N-boc propyl bromide in the presence of potassium carbonate to give an alkylated version of Intermediate **2b**. Then, mono-reduced intermediate **3c** was further brominated with PBr₃ giving Intermediate **4d**. This compound **4d** was alkylated on Py-crown compound which was synthesized by following the reported protocol in a separate step. Next, Boc deprotection is followed by hydrolysis afforded intermediate **6f**. Finally, **6f** was reacted with Bis PEG₄-TFP ester to obtain the activated TFP ester intermediate **7g**. All the intermediates were characterized by ¹H&¹³C-NMR and HRMS. The yields were mentioned below the arrow for each step. Py-Crown was synthesized as previously described (2). Bis-PEG₄-TFP is commercially available (Biopharma PEG).

Step 1: Synthesis of dimethyl 4-hydroxypyridine-2,6-dicarboxylate (2a**)**

Compound **2a** was synthesized according to the reported protocol (4).

Step 2: Synthesis of dimethyl 4-(3-((tert-butoxy carbonyl) amino)propoxy)pyridine-2,6-dicarboxylate (2b**)**

A mixture of Dimethyl 4-hydroxypyridine-2,6-dicarboxylate, **1a** (0.5 g, 2.37 mmol) and K₂CO₃ (0.64 g, 4.74 mmol) and tert-butyl (3-bromopropyl) carbamate (0.677 g, 2.84 mmol) in DMF (6 mL) was stirred at 70 °C under a Nitrogen (N₂) atmosphere for 12 h. The DMF was removed under reduced

pressure and water was added and extracted with ethyl acetate. The organic layer was dried over anhydrous sodium sulfate (Na_2SO_4) and concentrated under reduced pressure. The crude product was purified by column chromatography over silica gel (230-400 mesh) using 90%-100% EtOAc in hexane to give 0.78 g (90%) of compound **2b** as a white solid. ^1H NMR (400 MHz, DMSO-d_6): δ = 7.72 (s, 2H), 6.90-6.93 (m, 1H), 4.22 (t, J = 6 Hz, 2H), 3.91 (s, 6H), 3.09 (t, J = 6.4 Hz, 2H), 1.80-1.95 (m, 2H); 1.36 (s, 9H) ^{13}C NMR (100 MHz, DMSO-d_6): δ = 166.92, 165.09, 156.07, 149.79, 114.60, 78.01, 67.08, 53.16, 37.09, 29.20, 28.68; HRMS (m/z): 369.1661 [$\text{M} + \text{H}$] $^+$; Calc: 369.1584.

Step 3: Synthesis of methyl 4-(3-((tert-butoxycarbonyl)amino)propoxy)-6-(hydroxymethyl)picolinate (**3c**)

NaBH_4 (62 mg, 1.63 mmol) was added in two portions to a stirred solution of compound **2b** (0.5 g, 1.36 mmol) in DCM : MeOH (2:1, 20 mL) at room temperature (rt) under N_2 atmosphere and stirred for 3 h at rt. The reaction was quenched with sat. NH_4Cl and the solvents were removed under reduced pressure. The resulting residue was extracted into EtOAc, washed with brine solution, dried over anhydrous Na_2SO_4 and the organic layer was removed under reduced pressure. The crude product was purified by column chromatography over silica gel (230-400 mesh) using 5% methanol in EtOAc as an eluent to give 0.32 g (75%) of compound **3c** as off-white solid. ^1H NMR (400 MHz, DMSO-d_6): δ = 7.40 (d, J = 2.5 Hz, 1H), 7.20 (d, J = 2.0 Hz, 1H), 6.92 (s, 1H), 5.54 (t, J = 6 Hz, 1H), 4.56 (d, J = 6 Hz, 2H), 4.13 (t, J = 6.4 Hz, 2H), 3.86 (s, 3H), 3.09 (q, J = 6.4 Hz, 2H), 1.85 (q, J = 6.8 Hz, 2H), 1.37 (s, 9H); ^{13}C NMR (100 MHz, DMSO-d_6): δ = 166.52, 165.70, 164.91, 156.09, 148.73, 110.21, 109.68, 78.00, 66.35, 64.27, 55.38, 52.83, 37.10, 29.32, 28.69; HRMS (m/z): 341.1710 [$\text{M} + \text{H}$] $^+$; Calc: 341.1634.

Step 4: Synthesis of methyl 6-(bromomethyl)-4-(3-((tert-butoxycarbonyl)amino)propoxy)picolinate (**4d**)

A solution of PPh_3 (0.296 g, 1.12 mmol) was added in portion wise to a stirred solution of compound **3c** (0.32 g, 0.94 mmol), CBr_4 (0.374 g, 1.13 mmol) and K_2CO_3 (0.195 g, 1.42 mmol) in CH_2Cl_2 (25 mL) at 0°C (under N_2) and stirred for 1 h at rt. The reaction mixture was concentrated under reduced pressure and purified by column chromatography over silica gel (230-400 mesh) using 5% methanol in EtOAc as an eluent to give 0.28 g (75%) of compound **4d** as a white solid. ^1H NMR (400 MHz, CDCl_3): δ = 7.58 (d, J = 2.4 Hz, 1H), 7.16 (d, J = 2.0 Hz, 1H), 4.57 (s, 2H), 4.14 (t, J = 6.4 Hz, 2H), 3.99 (s, 3H), 3.33 (q, J = 6.4 Hz, 2H), 2.02 (t, J = 6.4 Hz, 2H), 1.43 (s, 9H); ^{13}C NMR (100 MHz, CDCl_3): δ = 166.59, 165.34, 158.86, 155.96, 149.22, 113.17, 111.27,

79.51, 66.28, 53.17, 37.50, 33.26, 29.35, 28.39; HRMS (m/z): 425.0681, 427.0661[M+Na]⁺; Calc: 427.0790.

Step 5: Synthesis of methyl 4-(3-((tert-butoxycarbonyl)amino)propoxy)-6-((16-((6-(methoxycarbonyl)pyridin-2-yl)methyl)-1,4,10,13-tetraoxa-7,16-diazacyclooctadecan-7-yl)methyl)picolinate (**5e**)

A mixture of the dark brown gummy solid, Py-crown (1 g, 2.44 mmol), compound **4d** (1.08 g, 2.68 mmol) and diisopropylethylamine (0.129 g, 6.1 mmol) in dry CH₃CN (100 mL) was stirred at 75° C for 12 h. The solvent was removed and purified by column chromatography over neutral alumina using 5-10% methanol in dichloromethane as an eluent to give 1.1 g of compound **5e** as brown viscous liquid. ¹H NMR (400 MHz, CDCl₃): δ= 7.93 (t, *J* = 7.2 Hz, 1H), 7.89 (d, *J* = 7.6 Hz, 1H), 7.77 (d, *J* = 8 Hz, 1H), 7.49 (d, *J* = 2 Hz, 1H), 7.38 (d, 1H), 4.11 (d, *J* = 11.6 Hz, 2H), 3.98-3.97 (m, 8H), 3.89 (s, 2H), 3.64-3.58 (m, 16H), 3.31 (t, *J* = 2.8 Hz, 2H), 2.85 (t, *J* = 5.2 Hz, 8H), 2.00 (q, *J* = 6.4 Hz, 2H), 1.42 (s, 9H); ¹³C NMR (100 MHz, CDCl₃): δ= 166.38, 165.92, 163.24, 161.51, 155.99, 148.73, 147.02, 137.32, 132.04, 126.18, 123.42, 111.54, 110.53, 70.79, 69.87, 65.92, 61.56, 54.47, 52.97, 37.55, 29.33, 28.41; HRMS (m/z): 734.3962[M+H]⁺; Calc: 734.3898.

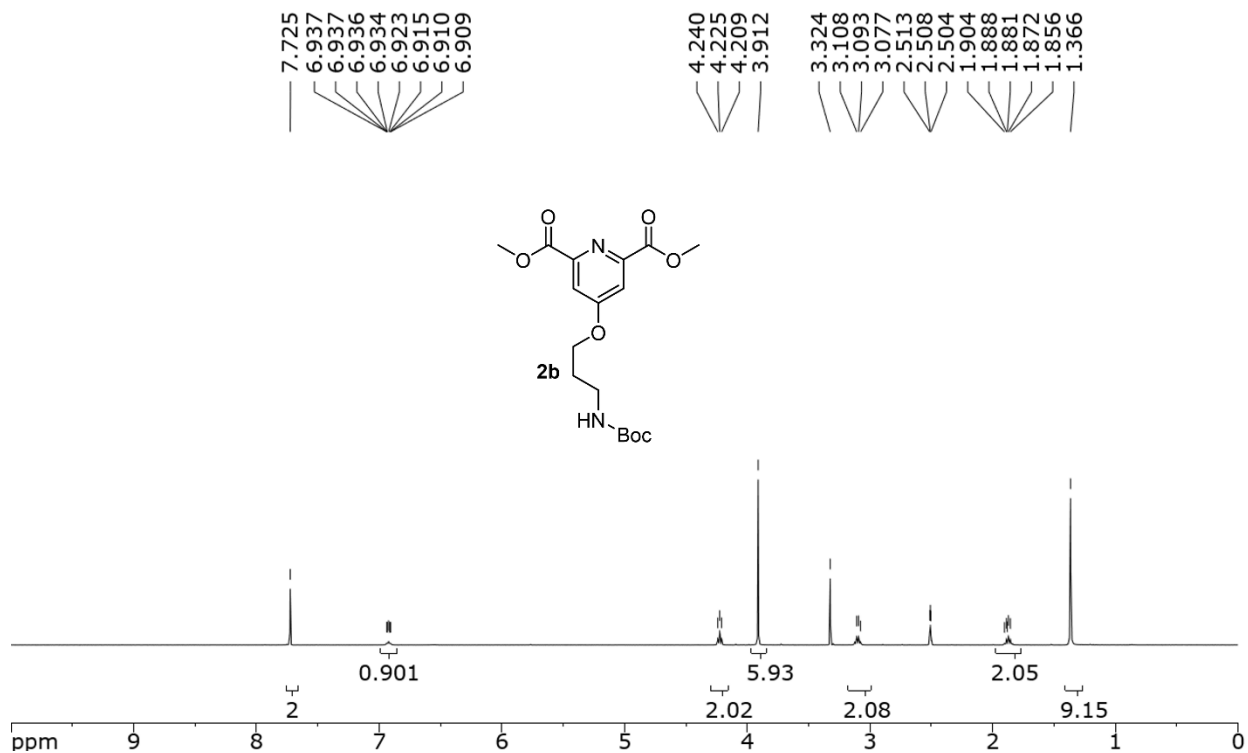
Step 6: Synthesis of 4-(3-aminopropoxy)-6-((16-((6-carboxypyridin-2-yl)methyl)-1,4,10,13-tetraoxa-7,16-diazacyclooctadecan-7-yl)methyl)picolinic acid (**6f**)

Compound **5e** (1.1 g, 1.50 mmol) was dissolved in aq. 6M HCl (15 mL) and stirred at room temperature for 3 h. After completion of the starting material (evidenced by LCMS), aq. HCl was removed under reduced pressure and the crude compound (1.4 g) was used in the next step of the synthesis without any further purification. The crude product was re-dissolved in THF: 2M LiOH (15: 15 mL) and stirred at rt for 12 h. The resulting crude product was purified by prep HPLC using Biotase SP4 system (see at the analytical methods), affording 1.1 g (69%) of compound **6f** as a pale brown solid. ¹H NMR (400 MHz, DMSO-d₆): δ= 8.15-8.09 (m, 2H), 7.95 (bs, 2H), 7.80 (q, *J* = 1.6 Hz, 1H), 7.61 (d, *J* = 2.4 Hz, 1H), 7.40 (d, *J* = 2.4 Hz, 1H), 4.72 (s, 2H), 4.63 (s, 2H), 4.26 (s, 2H), 3.86 (s, 8H), 3.58-3.55 (m, 16H), 3.01-2.96 (m, 2H), 2.07 (d, *J* = 4 Hz, 2H); ¹³C NMR (100 MHz, DMSO-d₆): δ= 166.78, 165.89, 158.93(TFA), 152.80, 151.42, 150.01, 148.18, 139.66, 128.33, 125.00, 118.15, 115.22, 114.47, 111.33, 111.30, 69.81, 66.26, 64.96, 57.21, 53.88, 36.54, 26.90; HRMS (m/z): 606.3141[M+H]⁺; Calc: 606.3061.

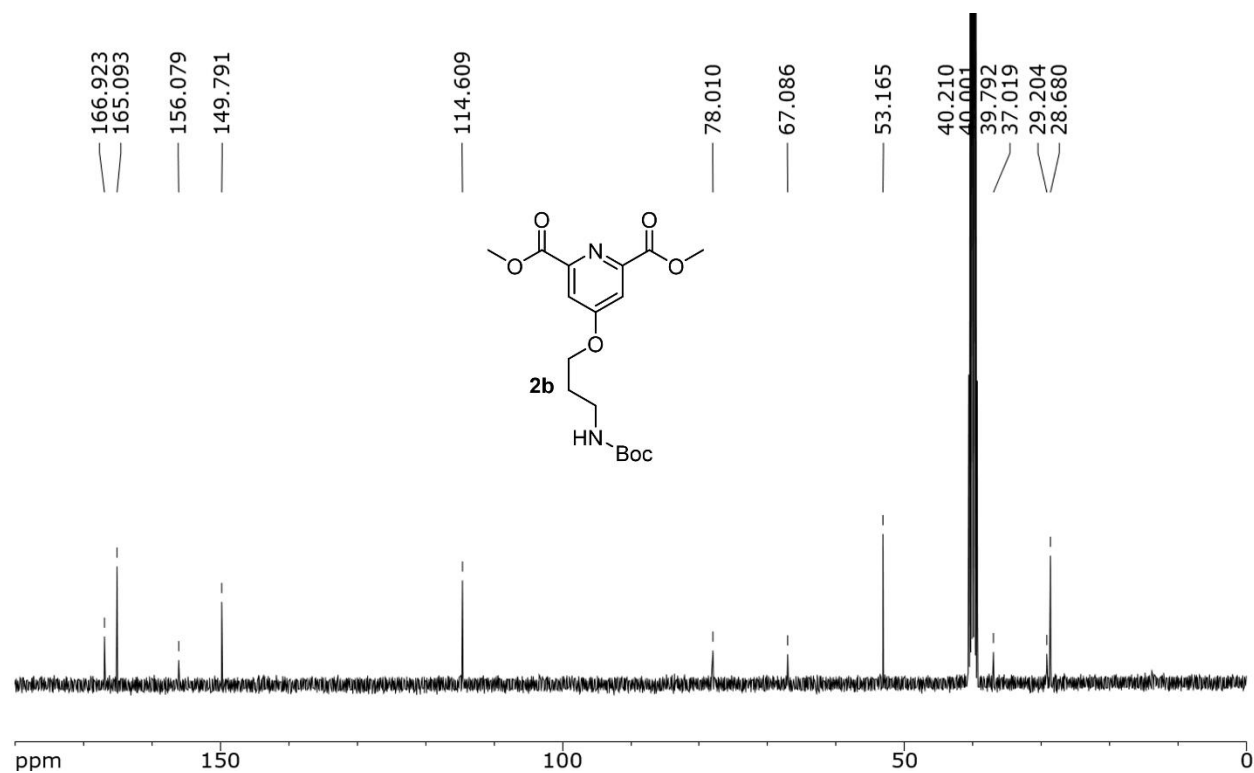
Step 7: Synthesis of Macropa-PEG₄-TFP ester (**7g**)

DIPEA (0.15 mL, 0.85 mmol) was added to a solution of compound **6f** (0.15 g, 0.14 mmol) and TFP-PEG₄-TFP (0.1 g, 0.17 mmol) in DMF (0.5 mL) at rt and stirred for 12 h at rt. Reaction

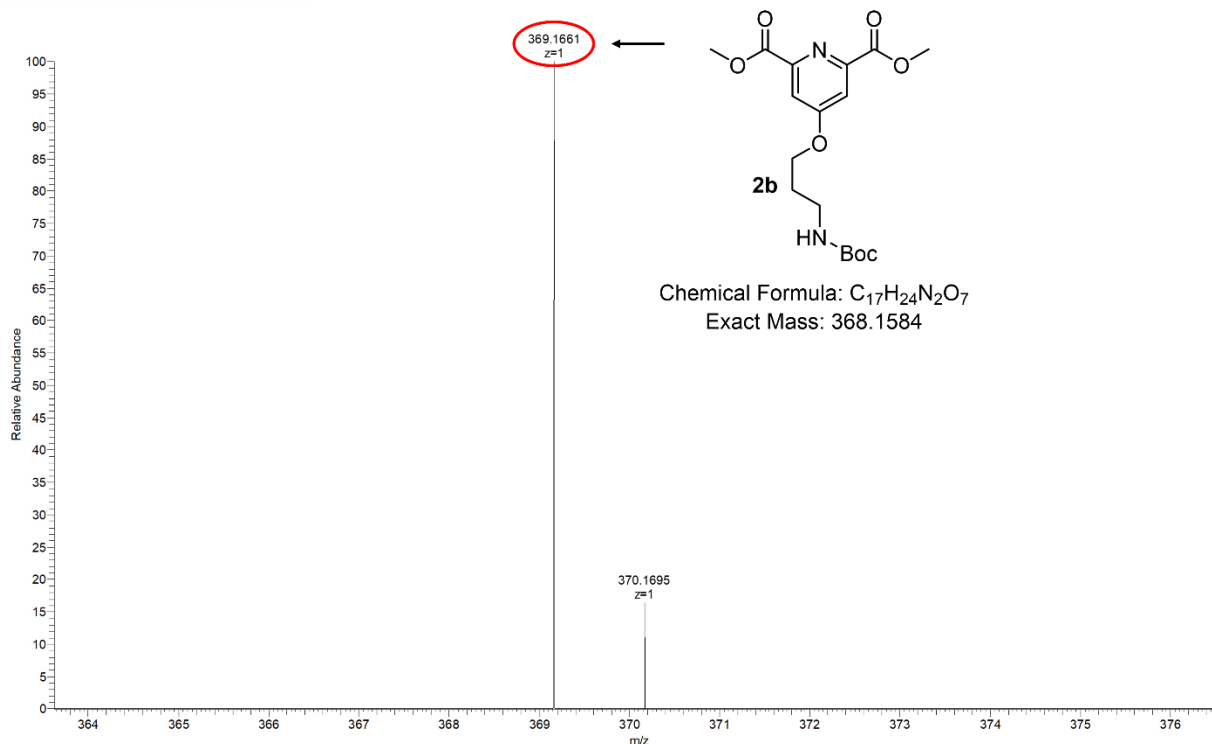
progress was monitored by LCMS. After completion of the reaction, the rm was directly purified by prep HPLC using Biotase SP4 (see at the analytical methods) to afford compound 7g (61 mg, 41%) as gummy solid. ¹H NMR (400 MHz, DMSO-d₆): δ= 8.13 (q, J = 7.2 Hz, 2H), 7.96 (q, J = 4.4 Hz, 1H), 7.80 (q, J = 1.6 Hz, 1H), 7.58 (d, J = 2 Hz, 1H), 7.38 (d, J = 2.4 Hz, 1H), 4.72 (s, 2H), 4.62 (s, 2H), 4.20 (t, J = 6.4 Hz, 2H), 3.86 (d, J = 4.4 Hz, 8H), 3.77 (m, J = 6 Hz, 2H), 3.58-3.47 (m, 30H), 3.22 (q, J = 6.8 Hz, 2H), 3.03 (t, J = 5.6 Hz, 2H), 2.30 (q, J = 6.4 Hz, 2H), 1.90 (q, J = 6.4 Hz, 2H); ¹³C NMR (100 MHz, DMSO-d₆): δ= 170.59, 168.36, 167.00, 165.88, 158.83(TFA), 151.44, 150.00, 148.18, 139.66, 128.22, 124.99, 118.28, 115.34, 114.52, 111.14, 104.91(TFA), 70.24, 69.95, 67.27, 66.02, 64.96, 57.21, 53.85, 35.61, 34.45, 28.99; ¹⁹F NMR (300 MHz, DMSO-d₆): δ= -74.21(tfa), -139.34, -153.33; HRMS (m/z): 1030.4263[M+H]⁺; Calc: 1030.4206.



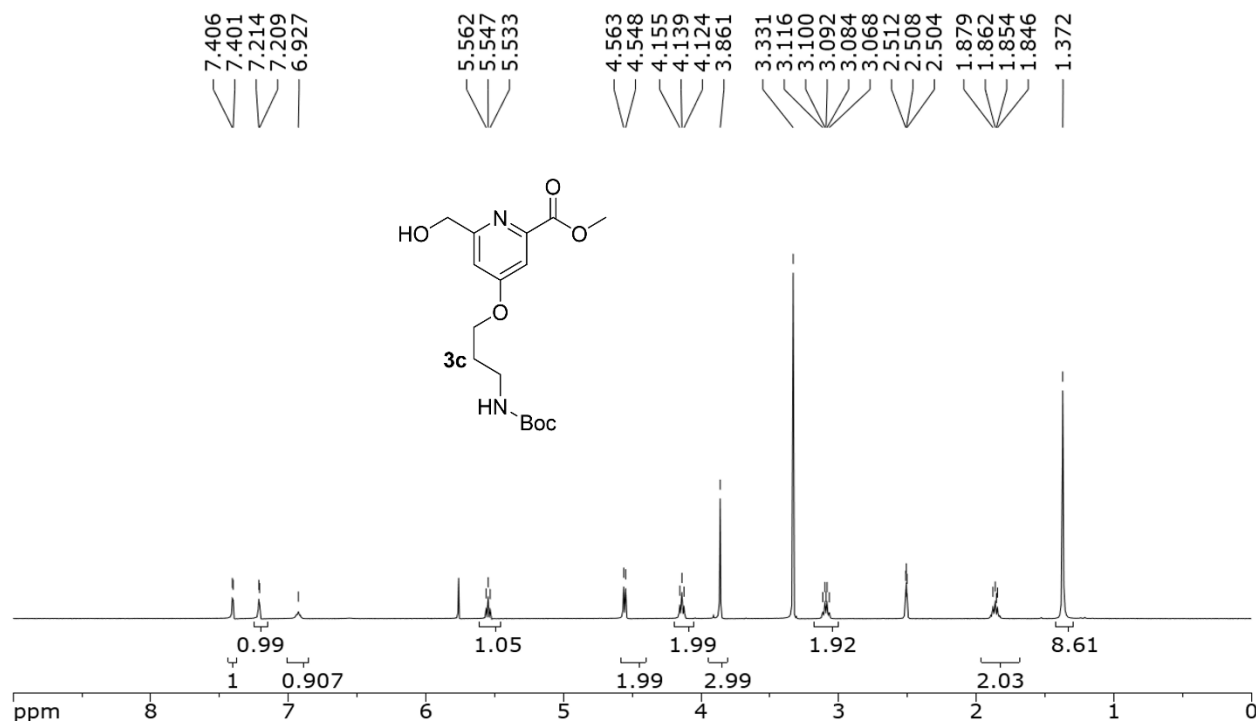
SUPPLEMENTAL FIGURE 19. ¹H NMR of compound **2b** in DMSO-d₆(400 MHz).



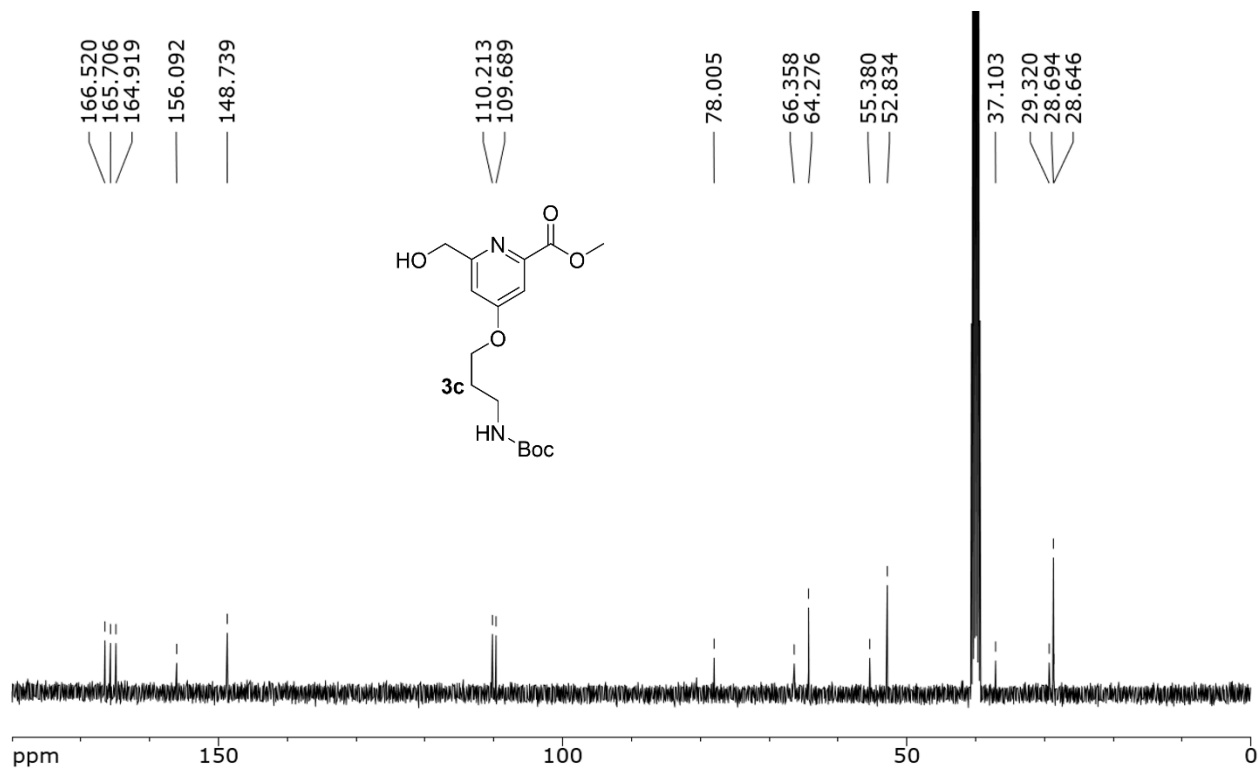
SUPPLEMENTAL FIGURE 20. ¹³C NMR of compound **2b** in DMSO-d₆(100 MHz).



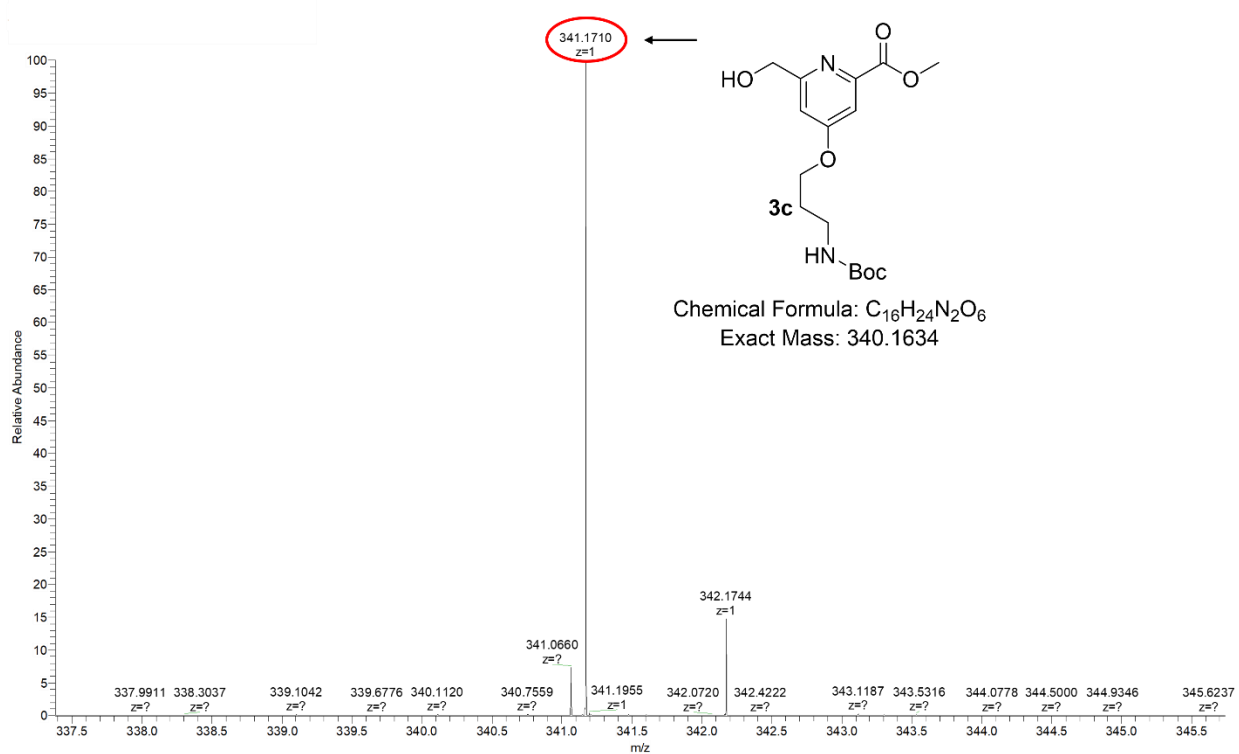
SUPPLEMENTAL FIGURE 21. HRMS of compound **2b**.



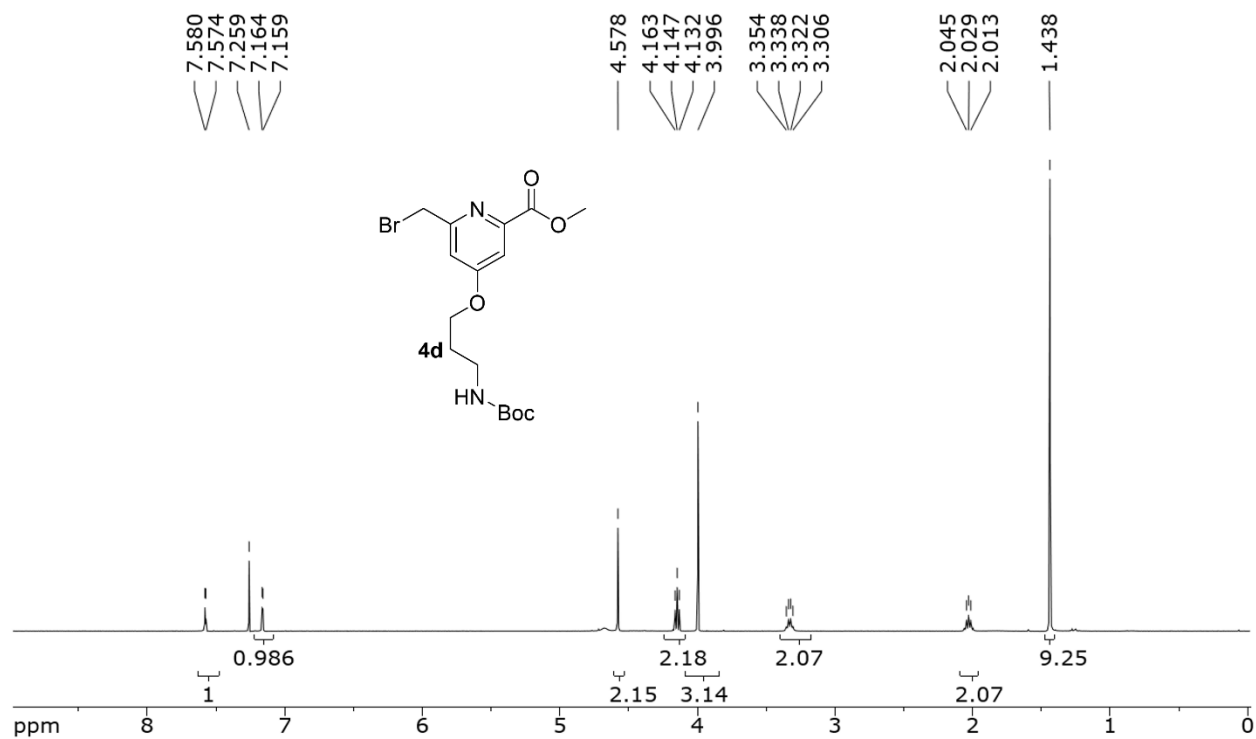
SUPPLEMENTAL FIGURE 22. ¹H NMR of compound **3c** in DMSO-d₆(400 MHz).



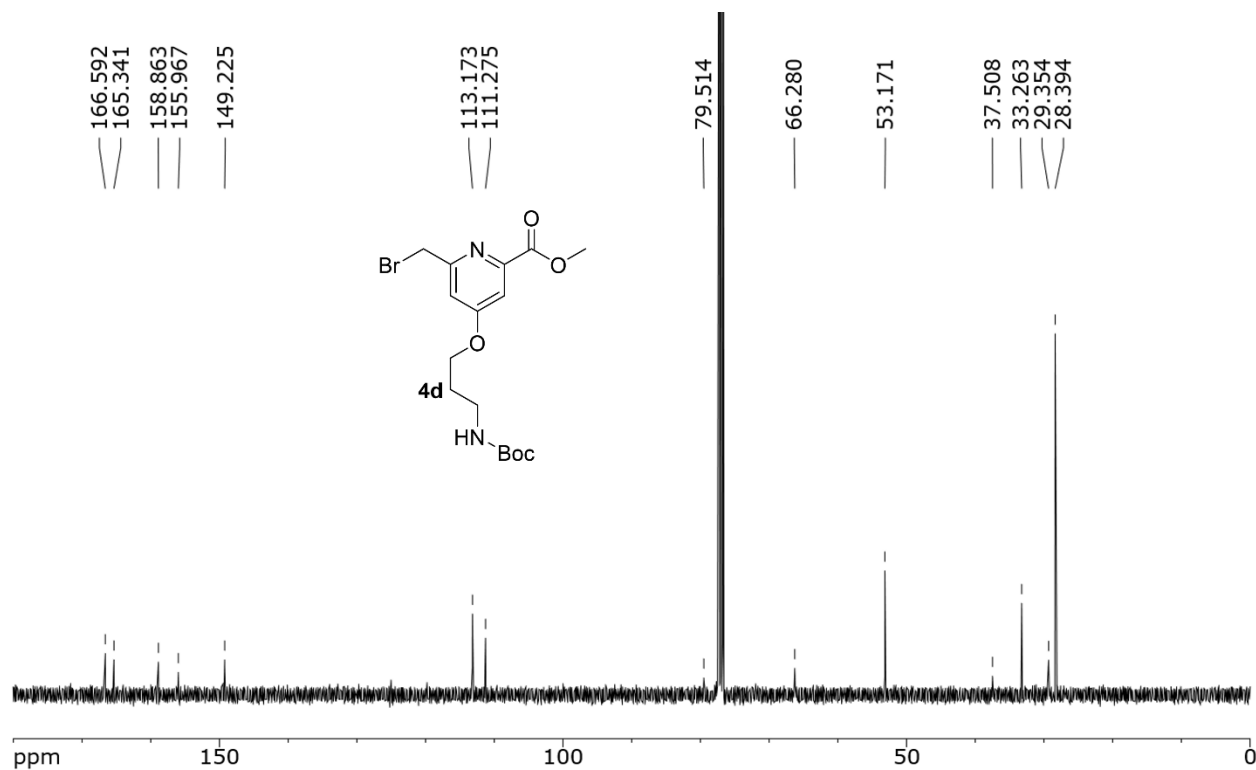
SUPPLEMENTAL FIGURE 23. ¹³C NMR of compound **3c** in DMSO-d₆ (100 MHz).



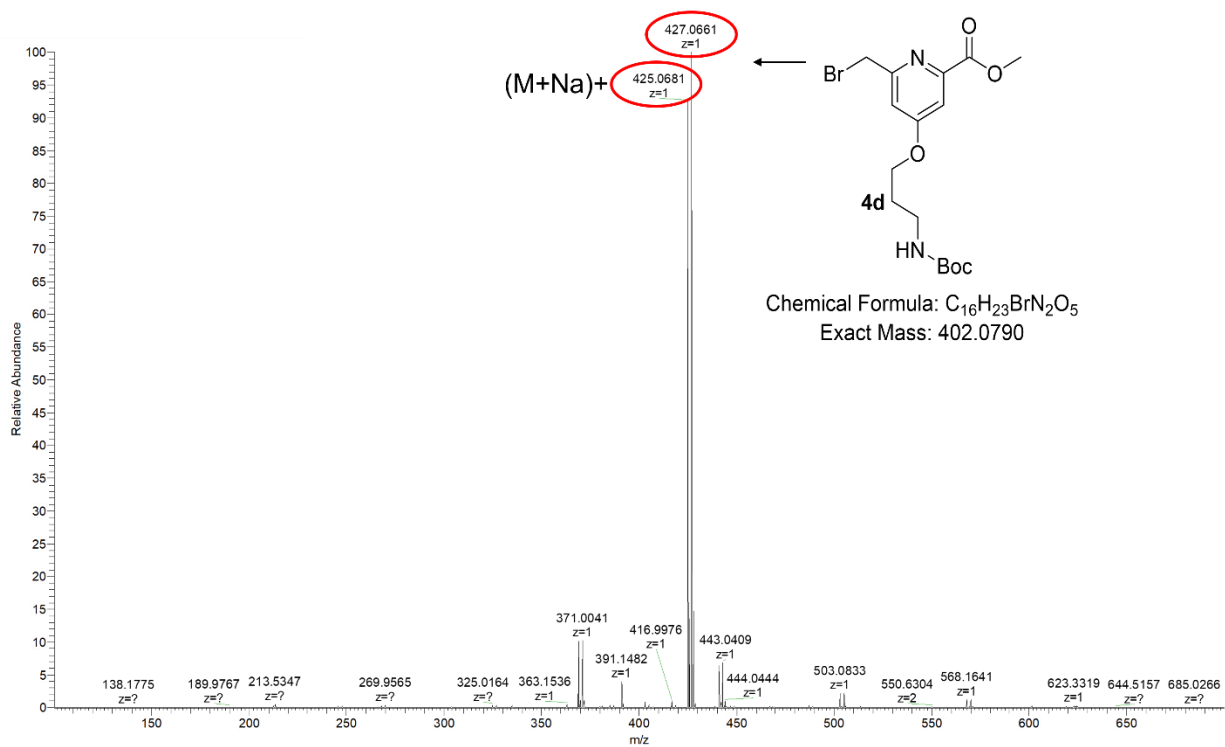
SUPPLEMENTAL FIGURE 24. HRMS of compound **3c**.



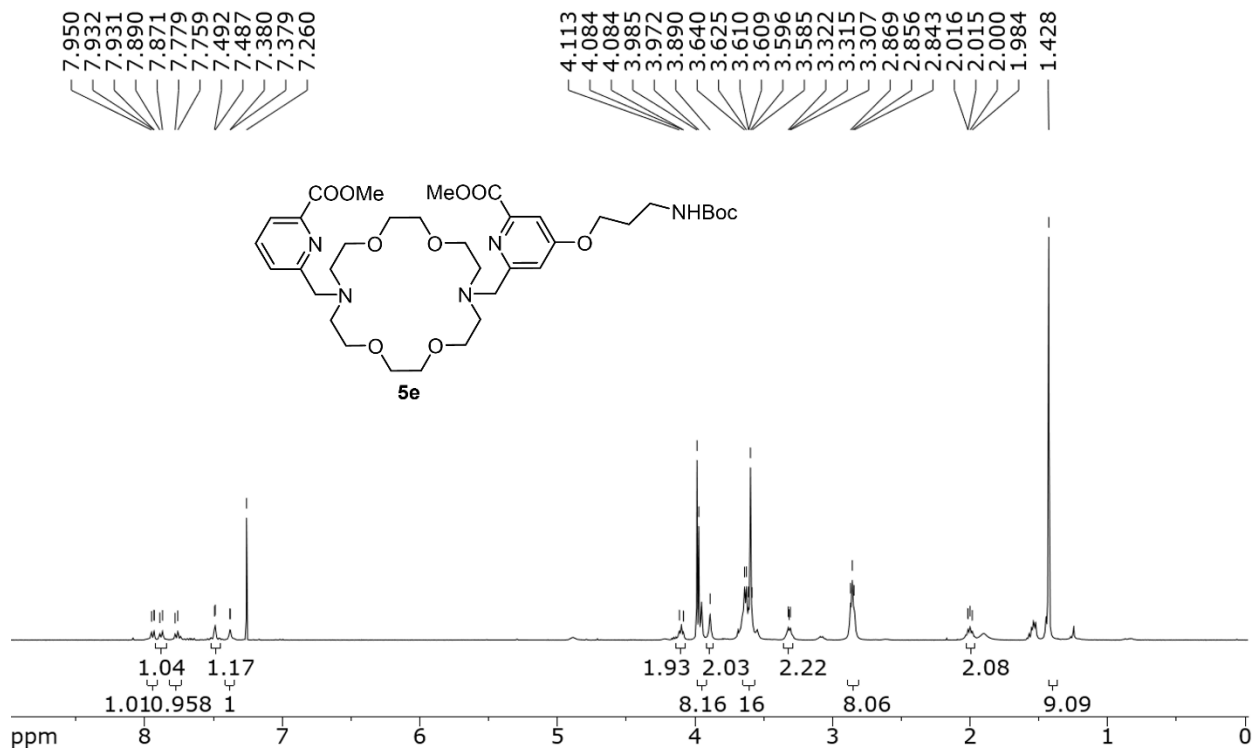
SUPPLEMENTAL FIGURE 25. ¹H NMR of compound **4d** in CDCl₃(400 MHz).



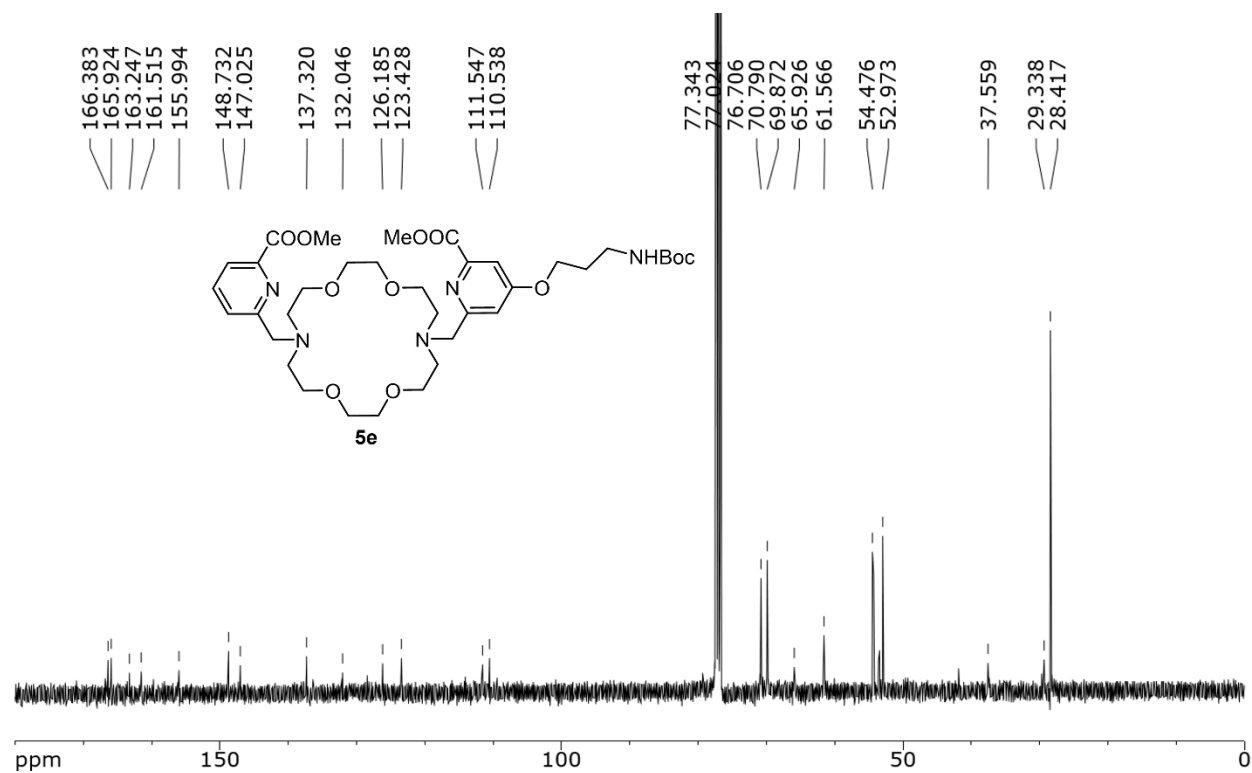
SUPPLEMENTAL FIGURE 26. ¹³C NMR of compound **4d** in CDCl₃(100 MHz).



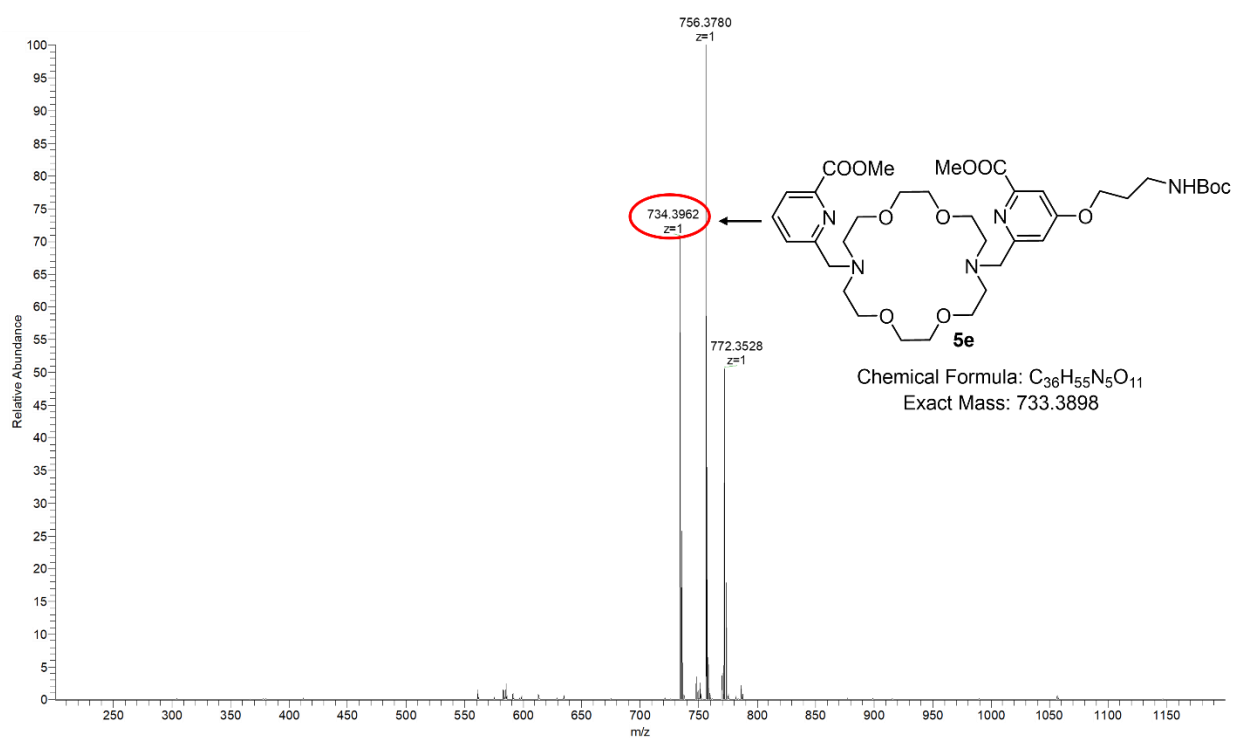
SUPPLEMENTAL FIGURE 27. HRMS of compound **4d**.



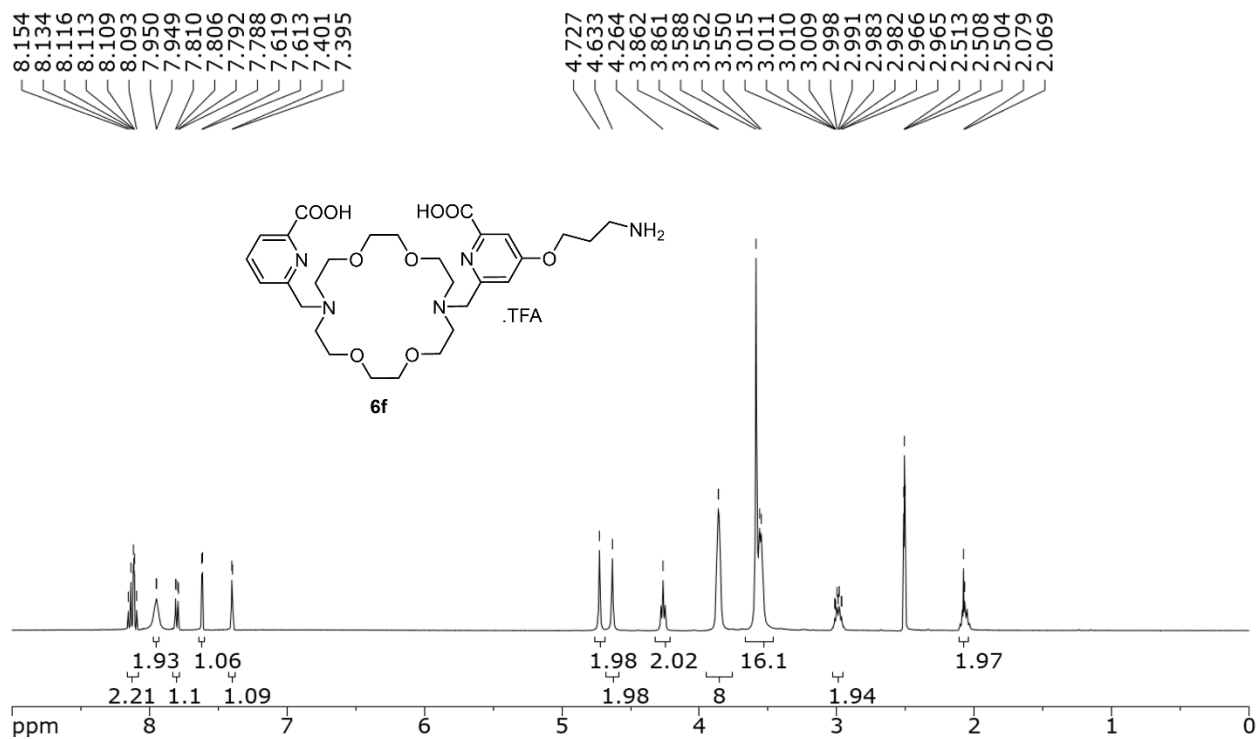
SUPPLEMENTAL FIGURE 28. ¹H NMR of compound **5e** in CDCl₃(400 MHz).



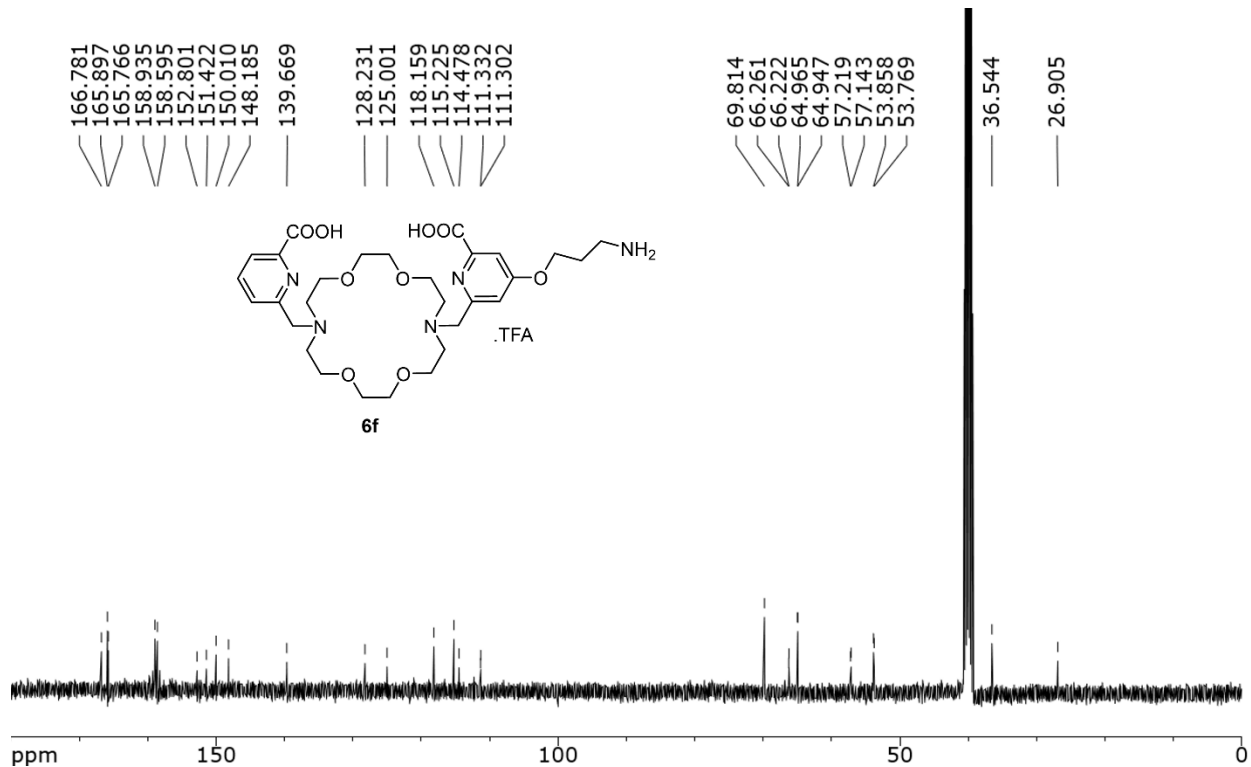
SUPPLEMENTAL FIGURE 29. ¹³C NMR of compound **5e** in CDCl₃(100 MHz).



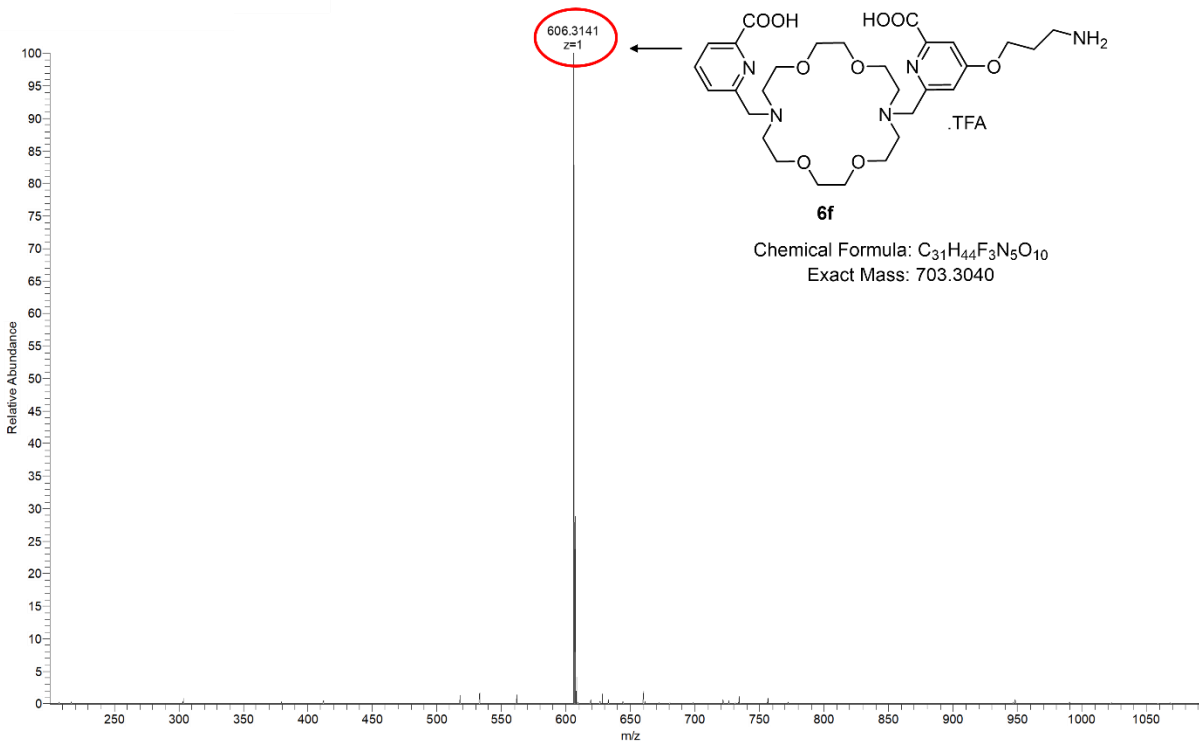
SUPPLEMENTAL FIGURE 30. HRMS of compound **5e**.



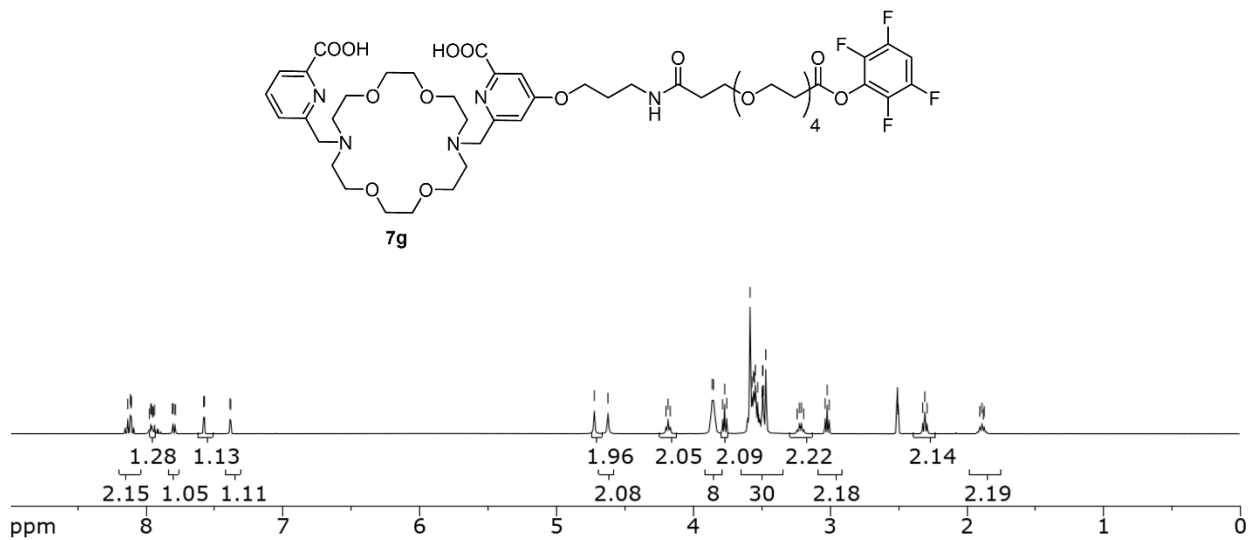
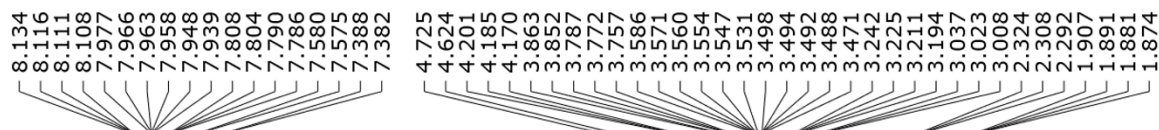
SUPPLEMENTAL FIGURE 31. ¹H NMR of compound **6f** in DMSO-d₆(400 MHz).



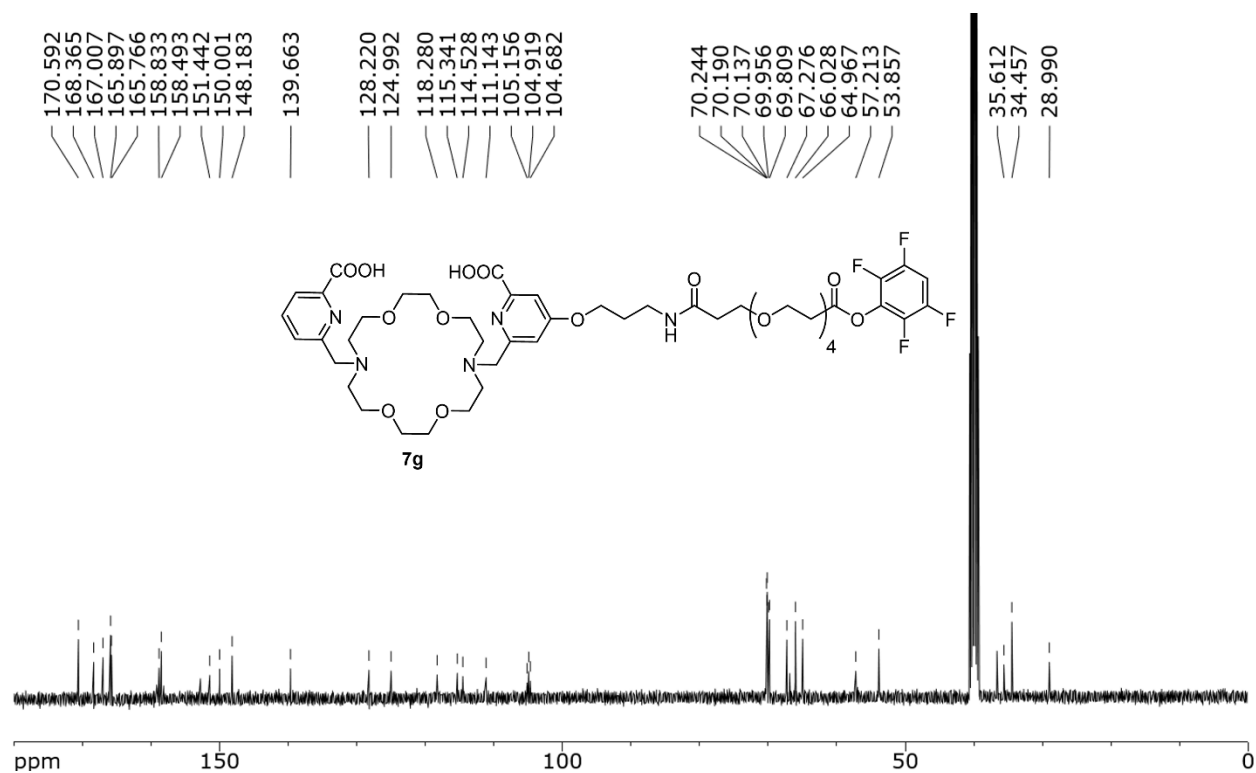
SUPPLEMENTAL FIGURE 32. ¹³C NMR of compound **6f** in DMSO₆(100 MHz).



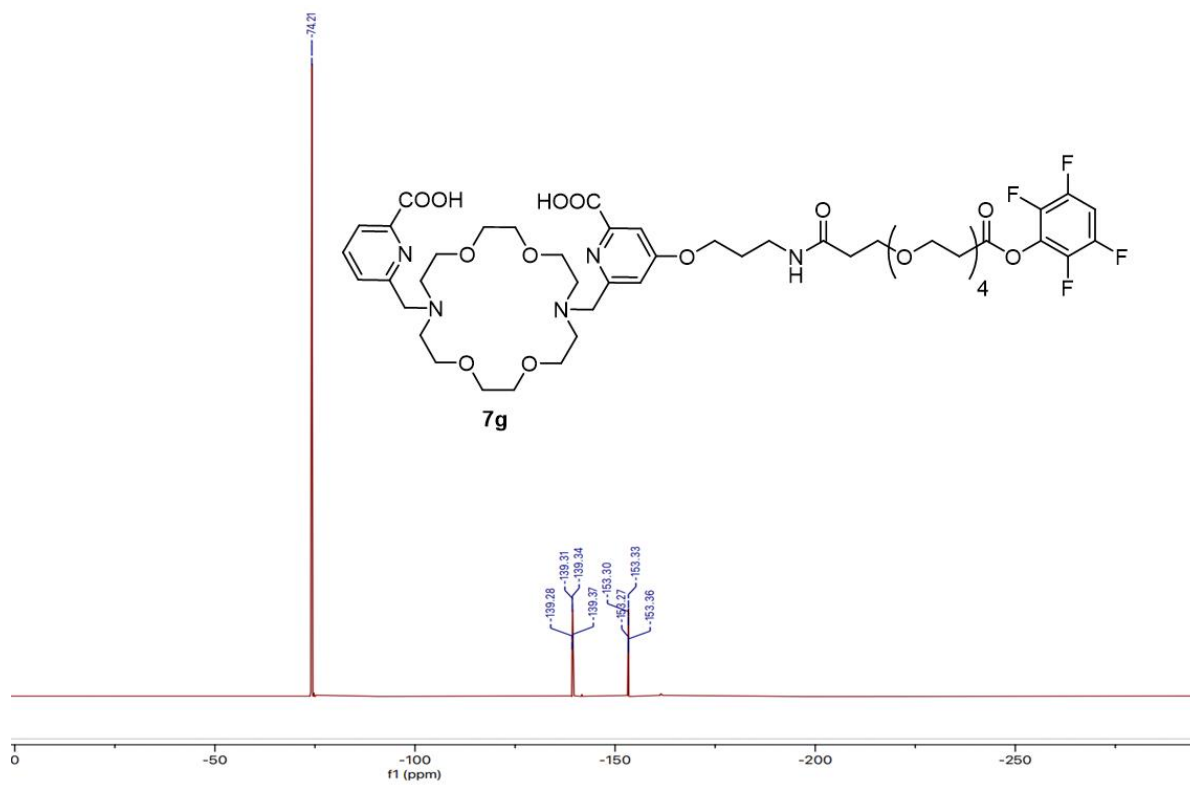
SUPPLEMENTAL FIGURE 33. HRMS of compound **6f**.



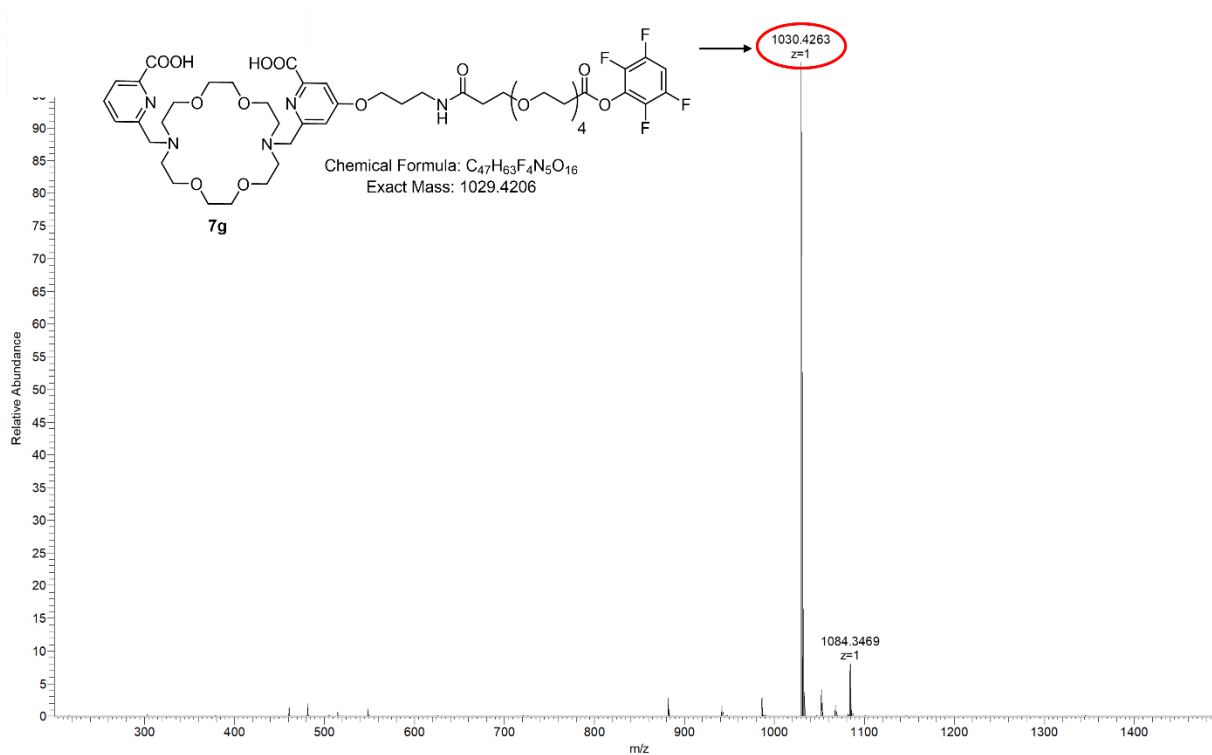
SUPPLEMENTAL FIGURE 34. ¹H NMR of compound **7g** in DMSO-d₆(400 MHz).



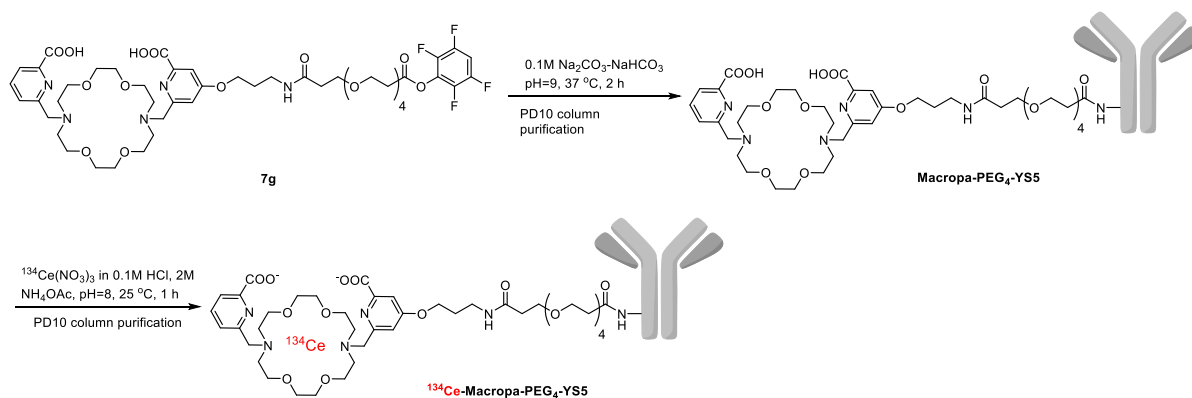
SUPPLEMENTAL FIGURE 35. ^{13}C NMR of compound **7g** in DMSO- d_6 (100 MHz).



SUPPLEMENTAL FIGURE 36. ^{19}F NMR of compound **7g** in DMSO- d_6 (300 MHz).



SUPPLEMENTAL FIGURE 37. HRMS of compound **7g**.



Supplemental Reaction Scheme 3: Synthesis and radiolabeling of Macropa-PEG₄-YS5.

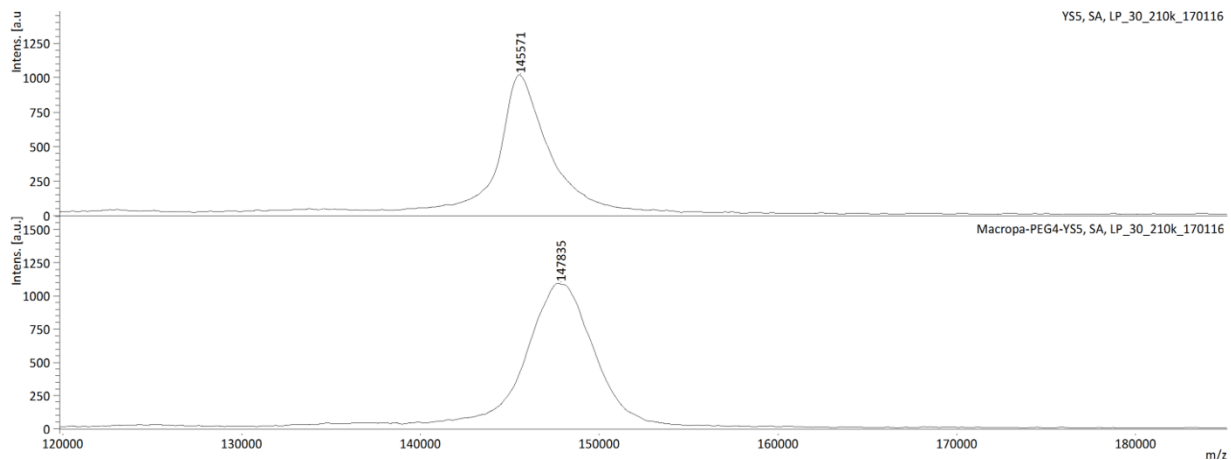
Antibody conjugation

The antibody conjugation was prepared using a modification of our previously described method (3). Briefly, 1 mg of YS5 in HEPES buffer was exchanged with 0.1 mol/L $Na_2CO_3-NaHCO_3$ buffer (400 μ L), pH 9 for three times using YM30K MW centrifugal filter unit (Millipore, MA, USA). The concentration of buffer exchanged YS5 was estimated as \sim 1.0 mg (60 μ L) using nanodrop one

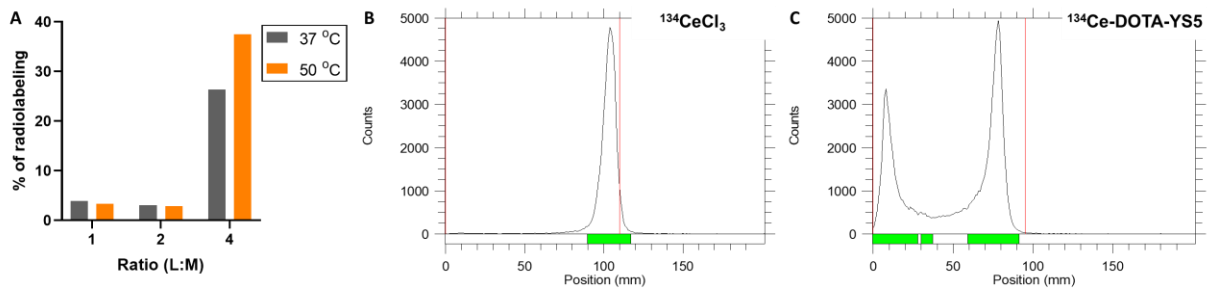
(Thermo scientific). The final volume is adjusted to 5 mg/mL with the same buffer. A stock solution of Macropa-PEG₄-TFP ester (2 mg/100 μL) was prepared and stored at -20 °C. Then, the YS5 antibody was incubated with Macropa-PEG₄-TFP ester (5.2 μL, 15 eq.) at 37 °C for 2 h. The conjugation mixture was purified over PD10 gel column filtration (GE healthcare) by eluting with 0.25M NaOAc (pH=6) as a mobile phase. Similarly, p-SCN-Bn-DOTA was conjugated with human antibody, YS5; ~2.6 PEG₄-Macropa (Supplemental Figure 31) & ~8.5 DOTA per YS5 (5) was confirmed by MALDI-ToF mass analysis.

Radiolabeling of Macropa-PEG₄-YS with Ac-225

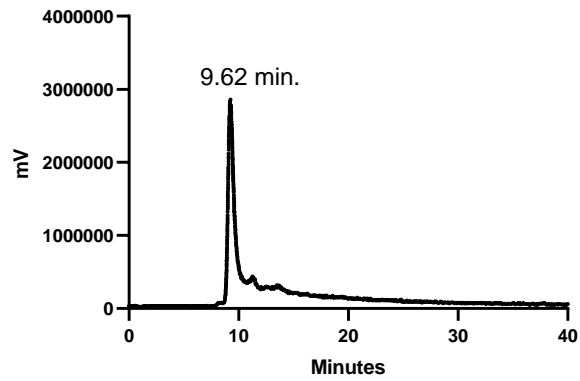
120 μg of Macropa-PEG₄-YS5 conjugate was mixed with 925 KBq (5.1 μL) of ²²⁵Ac(NO₃)₃ in 0.2M HCl in 2M NH₄OAc (30 μL, pH=5.8) buffer and L-Ascorbic acid (20 μL, 150 mg/mL) at 25 °C for 30 min. The radiolabeling progress was monitored by radio TLC by eluting with a mobile phase 10mM EDTA (pH=5.5) on iTLC-SG. The radiochemical yield was found to be 97.16%. Then, the radio Immunoconjugate was buffer exchanged with 0.9% saline (300 μL) by centrifugal filtration (YM30K molecular weight cut off) using Fisher scientific accuspun Micro 17R centrifuge. It was washed with 0.9% saline (400 μL) for two more times afforded 740 KBq (66.6%) of ²²⁵Ac-Macropa-PEG₄-YS5 with a radiochemical purity of 100%, with molar activity, 6.17 KBq/μg.



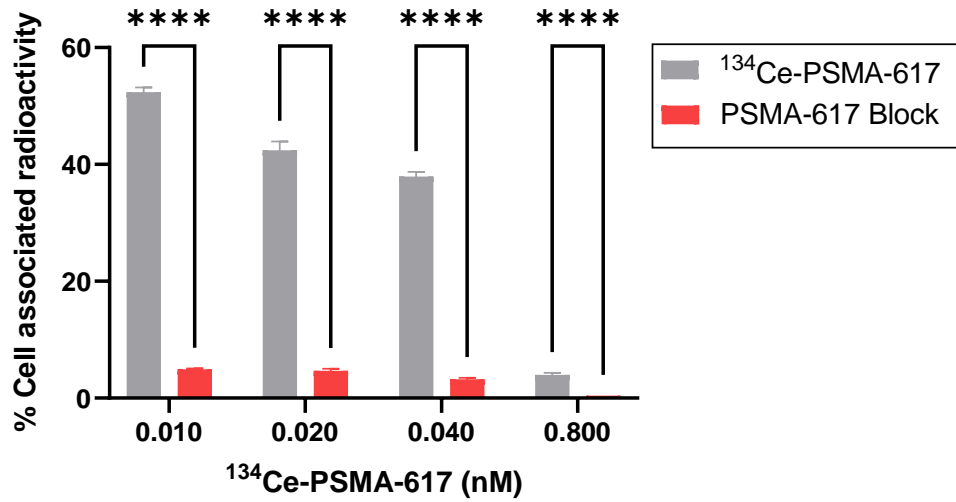
SUPPLEMENTAL FIGURE 38. MALDI-ToF mass analysis, YS5 and Macropa-PEG₄-YS5 chromatograms. Analysis confirms ~2.6 chelators per antibody. The mass difference between YS5 and Macropa-PEG₄-YS5 was divided by mass of Macropa-PEG₄ compound to yield the number of chelators per Antibody YS5.



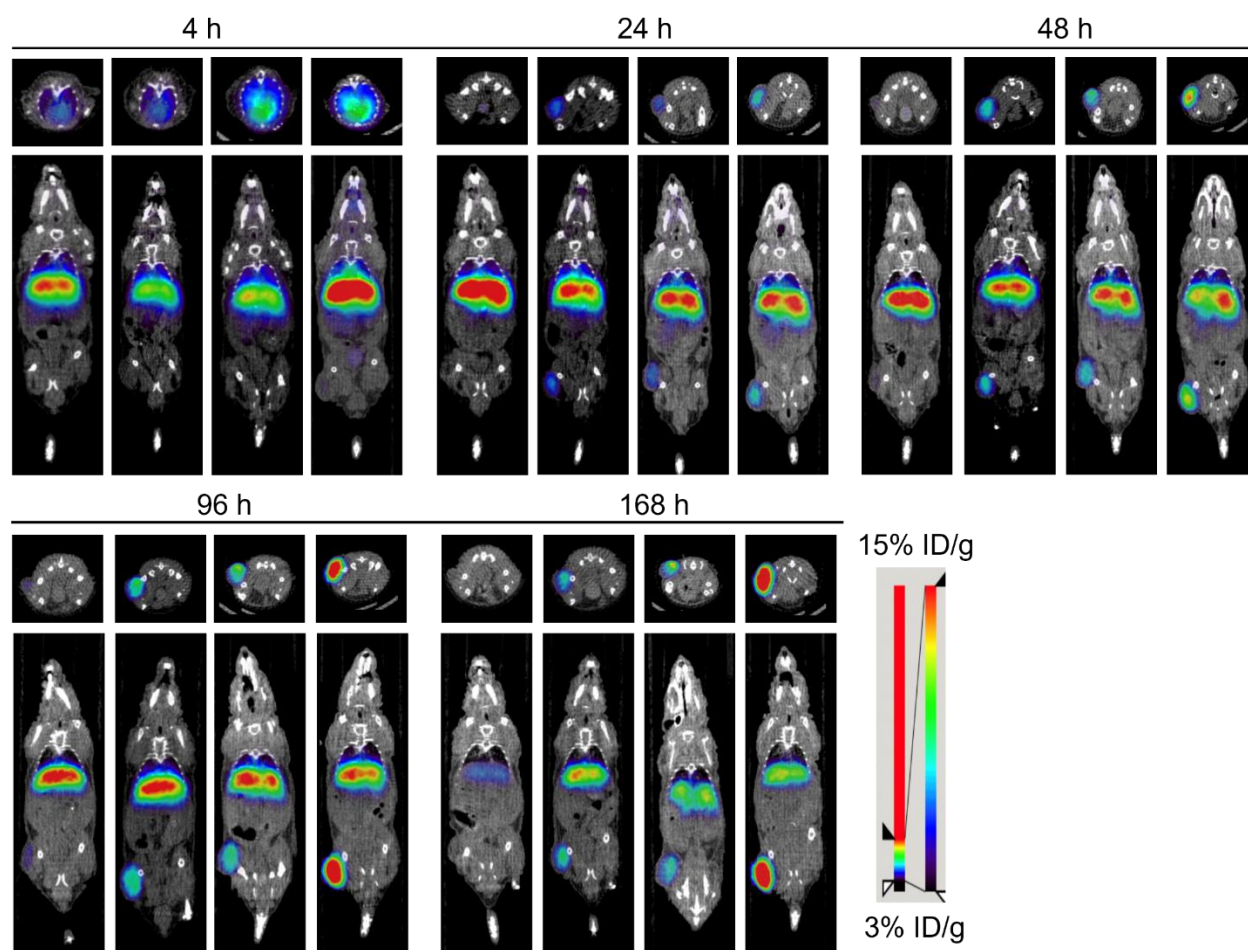
SUPPLEMENTAL FIGURE 39. Radiolabeling yields of DOTA-YS5 at increasing molar ratios (A); radio iTLC-SG of $^{134}\text{CeCl}_3$ (B), and $^{134}\text{Ce-DOTA-YS5}$ (C).



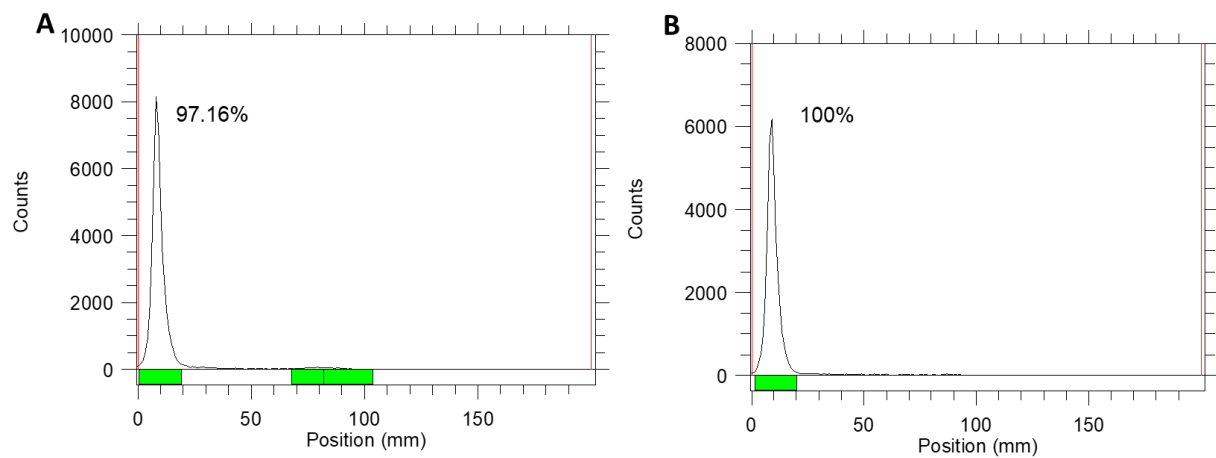
SUPPLEMENTAL FIGURE 40. Size exclusive chromatogram of chromatogram of $^{225}\text{Ac-Macropa-PEG}_4\text{-YS5}$, showing tailing in baseline between 9.62 min and 25 min.



SUPPLEMENTAL FIGURE 41. Cell binding assay of $^{134}\text{Ce-PSMA-617}$ on the 22Rv1 cell line (n = 3 per group). Error bars represent the standard deviation (SD); **** P < 0.0001; [52.38±0.65% Vs 4.92±0.11%; 42.44±1.19 Vs 4.69±0.28%; 37.97±0.65 Vs 3.21±0.22%; 3.97±0.27% Vs 0.44±0.008%]



SUPPLEMENTAL FIGURE 42. μ PET transverse (top) and coronal (bottom) Images acquired after administration of ^{134}Ce -Macropa-PEG₄-YS5 in 22Rv1 tumor bearing mice up to 168 h (n=4).



SUPPLEMENTAL FIGURE 43. Radio iTLC-SG of ^{225}Ac -Macropa-PEG₄-YS5 after 30 min incubation (A), After purification (B). A small aliquot (1 μL) was spotted on iTLC-SG and eluted with 10mM EDTA, pH=5.5; Immediately scanned after elution.

SUPPLEMENTAL TABLE 1: Ex vivo biodistribution of $^{134}\text{CeCl}_3$ at 1 and 24 h p.i., ^{134}Ce -Macropa.NH₂ at 1 h p.i., and ^{134}Ce -DOTA at 1 h p.i. (n = 3, mean \pm SD, n=2 for $^{134}\text{CeCl}_3$ 1 h).

Organ	$^{134}\text{CeCl}_3$		^{134}Ce -Macropa.NH ₂	^{134}Ce -DOTA
	1 h	24 h	1 h	1 h
Liver	22.79 \pm 1.75	21.63 \pm 2.63	0.80 \pm 0.15	0.44 \pm 0.13
Heart	2.38 \pm 0.43	1.54 \pm 0.72	0.49 \pm 0.14	0.43 \pm 0.27
Kidney	3.77 \pm 1.05	2.13 \pm 0.22	3.82 \pm 1.67	3.94 \pm 1.66
Lung	2.26 \pm 0.41	1.44 \pm 0.08	0.81 \pm 0.18	0.65 \pm 0.40
Spleen	1.26 \pm 0.34	2.32 \pm 0.81	0.32 \pm 0.04	0.36 \pm 0.11
Pancreas	0.64 \pm 0.17	0.39 \pm 0.10	0.19 \pm 0.03	0.19 \pm 0.12
Stomach	0.97 \pm 0.15	0.77 \pm 0.16	0.45 \pm 0.12	0.12 \pm 0.05
Small Int.	1.64 \pm 0.35	0.58 \pm 0.19	0.74 \pm 0.61	0.49 \pm 0.34
Large Int.	0.73 \pm 0.03	0.44 \pm 0.12	1.07 \pm 0.74	0.51 \pm 0.31
Brain	0.20 \pm 0.07	0.05 \pm 0.02	0.08 \pm 0.01	0.08 \pm 0.03
Muscle	0.59 \pm 0.36	0.13 \pm 0.01	0.38 \pm 0.19	0.25 \pm 0.11
Bone	13.06 \pm 0.40	12.83 \pm 2.92	0.39 \pm 0.09	0.32 \pm 0.13
Blood	0.61 \pm 0.20	0.02 \pm 0.01	0.86 \pm 0.19	1.07 \pm 0.80

SUPPLEMENTAL TABLE 2: Ex vivo biodistribution of $^{225}\text{AcCl}_3$, $^{225}\text{Ac-Macropa.NH}_2$ and $^{225}\text{Ac-DOTA}$ at 1 h p.i. (n = 3, mean \pm SD).

Organ	$^{225}\text{AcCl}_3$	$^{225}\text{Ac-Macropa.NH}_2$	$^{225}\text{Ac-DOTA}$
Liver	38.33 \pm 6.75	0.74 \pm 0.19	0.28 \pm 0.08
Heart	12.9 \pm 1.11	0.26 \pm 0.09	0.24 \pm 0.14
Kidney	14.44 \pm 1.44	3.54 \pm 1.07	3.07 \pm 0.99
Lung	6.03 \pm 0.39	0.65 \pm 0.28	0.36 \pm 0.09
Spleen	4.52 \pm 1.34	0.42 \pm 0.18	0.05 \pm 0.06
Pancreas	2.31 \pm 0.19	0.34 \pm 0.16	0.08 \pm 0.15
Stomach	2.62 \pm 0.80	0.53 \pm 0.30	0.22 \pm 0.15
Small Int.	4.44 \pm 0.47	0.96 \pm 1.01	0.41 \pm 0.29
Large Int.	3.52 \pm 1.04	3.11 \pm 2.71	0.52 \pm 0.15
Brain	0.63 \pm 0.17	0.08 \pm 0.08	0.05 \pm 0.05
Muscle	1.77 \pm 0.48	0.25 \pm 0.17	0.06 \pm 0.06
Bone	29.56 \pm 2.40	0.45 \pm 0.24	2.26 \pm 0.56
Blood	2.55 \pm 0.74	0.32 \pm 0.08	0.23 \pm 0.02

SUPPLEMENTAL TABLE 3: Ex vivo biodistribution of ^{134}Ce -Macropa-PEG₄-YS5 at 7 days (n=5), 14 days (n=2) and ^{225}Ac -Macropa-PEG₄-YS5 at 7 days (n=4) in athymic nu/nu mice bearing 22Rv1 tumors subcutaneously (mean \pm SD).

Organ	^{134}Ce -Macropa-PEG ₄ -YS5		^{225}Ac -Macropa-PEG ₄ -YS5
	7 days	14 days	7 days
Liver	21.59 \pm 0.35	14.48 \pm 2.39	2.37 \pm 0.35
Heart	1.89 \pm 0.81	0.65 \pm 0.08	2.09 \pm 0.57
Kidney	4.69 \pm 0.94	1.81 \pm 0.09	5.07 \pm 1.68
Lung	3.86 \pm 0.92	1.68 \pm 0.04	2.55 \pm 0.47
Spleen	7.22 \pm 1.73	1.68 \pm 0.04	1.53 \pm 0.12
Pancreas	0.54 \pm 0.10	0.25 \pm 0.04	0.80 \pm 0.07
Stomach	0.58 \pm 0.09	0.50 \pm 0.03	0.28 \pm 0.11
Small Int.	1.13 \pm 0.13	0.77 \pm 0.58	0.96 \pm 0.27
Large Int.	0.87 \pm 0.20	0.23 \pm 0.10	0.70 \pm 0.09
Brain	0.16 \pm 0.04	0.10 \pm 0.003	0.28 \pm 0.11
Muscle	0.60 \pm 0.12	0.28 \pm 0.01	0.53 \pm 0.04
Bone	4.61 \pm 1.21	4.84 \pm 0.28	1.49 \pm 0.27
Blood	4.66 \pm 1.25	1.42 \pm 0.28	3.95 \pm 0.75
Tumor	37.17 \pm 7.32	33.11 \pm 9.27	34.75 \pm 7.86

REFERENCES:

1. Su Y, Liu Y, Behrens CR, Bidlingmaier S, Lee NK, Aggarwal R, et al. Targeting CD46 for both adenocarcinoma and neuroendocrine prostate cancer. *JCI insight*. 2018;3(17) e121497.
2. Thiele NA, Brown V, Kelly JM, Amor-Coarasa A, Jermilova U, MacMillan SN, et al. An Eighteen-Membered Macrocyclic Ligand for Actinium-225 Targeted Alpha Therapy. *Angew Chem Int Ed Engl*. 2017;56:14712-7.
3. Wang S, Li J, Hua J, Su Y, Beckford-Vera DR, Zhao W, et al. Molecular Imaging of Prostate Cancer Targeting CD46 Using ImmunoPET. *Clin. cancer res*. 2021;27:1305-15.
4. Chauvin A, Tripier R, Bünzli J. A new versatile methodology for the synthesis of 4-halogenated-6-diethylcarbamoylepyridine-2-carboxylic acids. *Tetrahedron Letters*. 2001;42:3089-91.